12-3-2014 12:00 AM

Influence of Water Chemistry Parameters on the Dissolution Rate of the Lead (II) Carbonate Hydrocerussite

Caitlin SE Kushnir, *The University of Western Ontario*

Supervisor: Dr. Clare Robinson, *The University of Western Ontario*
A thesis submitted in partial fulfillment of the requirements for the Master of Engineering
Science degree in Civil and Environmental Engineering
© Caitlin SE Kushnir 2014

INFLUENCE OF WATER CHEMISTRY PARAMETERS ON THE DISSOLUTION RATE OF THE LEAD (II) CARBONATE HYDROCERUSSITE

(Thesis format: Integrated Article)

By

Caitlin S. E. Kushnir

Graduate Program in Engineering Science,

Department of Civil and Environmental Engineering

A thesis submitted in partial fulfillment

of the requirements for a degree of

Master of Science

The School of Graduate and Postdoctoral Studies

The University of Western Ontario

London, Ontario, Canada

© Caitlin S. E. Kushnir, 2014

ABSTRACT

Lead is a toxic heavy metal and nominal exposure can have serious health impacts. The dissolution of lead from corrosion scales within lead service lines and lead bearing plumbing materials in water distribution systems is a major concern for municipalities around the world. Water utility operators have two options to protect public health, stabilization of the corrosion scale, or lead service line replacement. As replacement programs are slow and costly, corrosion control through scale stabilization by adjusting water chemistry parameters is generally the most accessible option for utility operators. Effective corrosion control requires critical understanding the composition of the corrosion scale and how components of the scale behave under different water conditions. Lead (II) carbonates are present and often in corrosion scales and may control total dissolved lead concentrations within typical drinking water systems under flowing water conditions and short stagnation periods. While the thermodynamic solubility of hydrocerussite has been investigated previously, very little is known about the dissolution rates of hydrocerussite.

This work examines the kinetic dissolution of the lead (II) carbonate hydrocerussite $(Pb_3(CO_3)_2(OH)_2)$ under four pH conditions (7.5, 8, 9, 10), three dissolved inorganic carbon concentrations (DIC; 10, 20, 50 mg C/L), and three initial hydrocerussite concentrations (10, 20, 50 mg/L) in batch experiments. Experiments were performed to determine total dissolved lead dissolution curves at short time scales (<2 hr). Equilibrium dissolved lead concentrations were achieved in less than 40 minutes, and were consistent with findings from previous studies – equilibrium total dissolved lead concentrations were highest for pH 7.5 and pH 10 and lowest for pH 9. The formation of cerussite may have interfered with the dissolution process at a pH 7.5. The equilibrium total dissolved lead concentrations decreased with increasing DIC. All

experimental equilibrium values were within the range of expected equilibrium concentrations simulated with the geochemical modelling program PHREEQC using combinations of solubility constants from literature for cerussite and hydrocerussite. These rate constants represent the largest source of error with respect to calculating equilibrium total dissolved lead. PHREEQC was used to speciate total dissolved lead equilibrium concentrations under experimental conditions to determine an approximate solubility product for hydrocerussite of -15.98 ± 0.53.

The kinetic dissolution data of total dissolved lead was evaluated by an integral approach. In general it was found that the dissolution rate constant increased with increasing pH, DIC and initial solid loading. The expressions describing how the kinetic rate constant determined under varying pH, DIC, and initial hydrocerussite conditions were combined into a rate expression. This kinetic dissolution expression matched the experimental data well and can be used to approximate total dissolved lead levels. These results provide a basis for further development of a kinetic-based lead corrosion scale dissolution model that utility operators may use to estimate how operational changes will affect dissolved lead concentrations in water distribution systems.

ACKNOWLEDGEMENTS

TABLE OF CONTENTS

LIST OF TABLES

LIST OF FIGURES

LIST OF APPENDICES

1   CHAPTER ONE: INTRODUCTION

Elevated lead levels in drinking water are a serious public health concern for many municipalities worldwide. Lead in drinking water is colorless, tasteless, and odorless with no indication of regulatory excess [1]. Drinking water contaminated with lead can cause acute toxic effects in anyone; however pregnant women and children under 6 years old are at the highest risk [1]. Exposure to lead through drinking water occurs due to the presence of lead-bearing plumbing materials in water distribution systems [2]. Programs targeted at removing lead service lines from distribution systems are progressing in many municipalities, but these programs are extremely expensive and very slow. Despite ongoing replacement programs, approximately 3.3 million lead service lines and 6.4 million lead service connections are still remaining in the mid-west and north-east of the United States alone [3].

Over time, an internal corrosion scale develops on the inside of lead service lines and by changing water chemistry parameters this corrosion scale can dissolve into drinking water [4]. Corrosion control strategies can be implemented by utility operators by changing the water chemistry to promote conditions within the service lines to prevent or reduce the dissolution of the internal corrosion scale. Destabilization of the corrosion scale and entrainment of lead in drinking water depends numerous factors including the length and diameter of lead service line, water chemistry, scale composition, water use patterns, and hydraulic flow regimes [5]. Control over many of these variables is impossible; however the most accessible one for utility operators to adjust is water chemistry. Water chemistry interacts with the corrosion scale solid phases to either stabilize or alternatively promote dissolution of the scale. A clear understanding of the corrosion scale composition and the influence of water chemistry parameters on the stability of the scale is required for utility operators to implement effective corrosion control strategies. The

corrosion scales on the interior of lead service lines are complex and are comprised primarily of lead (II) carbonates and lead (IV) oxides [6]. Lead (II) carbonates found within the scales are typically cerussite ($PbCO_3$) and hydrocerussite ($Pb_3(CO_3)_2(OH)_2$) [6]. These are more soluble than lead (IV) oxides and often control total dissolved lead levels under short stagnation times or flowing conditions [7]. The two key chemical parameters that often control the dissolution of the lead corrosion scale are pH and dissolved inorganic carbon (DIC) [4]. Additional chemical parameters which have been shown to affect the dissolution of various lead compounds are disinfectant type (e.g., chlorine, chloramines), manganese, phosphate, iodine, and natural organic matter (NOM) [8-13]. Over the last decade, research has focused on evaluating the equilibrium and kinetic behavior of lead (IV) oxides under various water chemistry conditions, and the subsequent impact on total dissolved lead in drinking water [11-30]. While the importance of lead (II) carbonates in controlling dissolved lead levels has been widely acknowledged, few studies have focused specifically on quantifying the equilibrium behavior or kinetic dissolution of these phases under different chemical conditions [23-27]. Since the lead (IV) carbonates may play a greater role in the dissolution of lead corrosion scales in water distribution systems, research is needed to quantify the behavior of these solid phases including their rate of dissolution under varying water chemistry conditions [31].

The objective of this work is to evaluate the kinetic dissolution of the lead (II) carbonate hydrocerussite under a range of pH and DIC conditions. Understanding how these key parameters influence the dissolution of hydrocerussite and developing a kinetic dissolution rate expression is essential to enable utility operators to approximate dissolved lead levels at the tap and to develop and implement effective corrosion control strategies.

REFERENCES

1. Health Canada. *Lead Information Package - Some Commonly Asked Questions About Lead and Human Health*. Environmental and Workplace Health 2014 2009-04-23 [cited 2014 September 2014]; Available from: www.hc-sc.gc.ca.
2. Government of Canada. *Reduce your exposure to lead*. Environmental Health 2014 2012-11-16 September 2014]; Available from: http://healthycanadians.gc.ca/.
3. American Water Works Association Research Foundation (AWWARF), *Distribution System Water Quality Changes Following Implementation of Corrosion Control Strategies.* American Water Works Association Research Foundation,, 2000.
4. Schock, M.R., *Response of lead solubility to dissolved carbonate in drinking water.* AWWA, 1980. **72**(12).
5. Sandvig, A., et al., *Contribution of service line and plumbing fixtures to lead and copper rule compliance issues*. 2008: Awwa Research Foundation.
6. Kim, E.J. and J.E. Herrera, *Characteristics of lead corrosion scales formed during drinking water distribution and their potential influence on the release of lead and other contaminants.* Environmental Science & Technology, 2010. **44**(16): p. 6054-6061.
7. Fabbricino, M. and G.V. Korshin, *Changes of the Corrosion Potential of Iron in Stagnation and Flow Conditions and Their Relationship with Metal Release.* Water Research, 2014.
8. Cantor, A.F., et al., *Effect of chlorine on corrosion in drinking water systems.* AWWA, 2003. **95**(5): p. 112-123.
9. Edwards, M. and A. Dudi, *Role of chlorine and chloramine in corrosion of lead-bearing plumbing materials.* AWWA, 2004. **96**(10): p. 69-81.
10. Vasquez, F.A., *The Effect of free chlorine and chloramines on lead release in a distribution system*. 2005, University of Central Florida Orlando, Florida.
11. Shi, Z. and A.T. Stone, *PbO2 (s, plattnerite) reductive dissolution by aqueous manganous and ferrous ions.* Environmental Science & Technology, 2009. **43**(10): p. 3596-3603.
12. Shi, Z. and A.T. Stone, *PbO2 (s, plattnerite) reductive dissolution by natural organic matter: Reductant and inhibitory subfractions.* Environmental Science & Technology, 2009. **43**(10): p. 3604-3611.
13. Wang, Y., J. Wu, and D.E. Giammar, *Kinetics of the Reductive Dissolution of Lead (IV) Oxide by Iodide.* Environmental Science & Technology, 2012. **46**(11): p. 5859-5866.
14. Cao, M., et al., *Selected-control synthesis of PbO2 and Pb3O4 single-crystalline nanorods.* Journal of the American Chemical Society, 2003. **125**(17): p. 4982-4983.
15. Foundation), W.W.R., *Lead(IV) Oxide Formation and Stability in Drinking Water Distribution Systems* Y.X. Yin Wang, and Daniel E. Giammar Editor. 2012.
16. Lin, Y.-P., M.P. Washburn, and R.L. Valentine, *Reduction of lead oxide (PbO2) by iodide and formation of iodoform in the PbO2/I-/NOM system.* Environmental Science & Technology, 2008. **42**(8): p. 2919-2924.
17. Lin, Y.-P. and R.L. Valentine, *Release of Pb (II) from monochloramine-mediated reduction of lead oxide (PbO2).* Environmental Science & Technology, 2008. **42**(24): p. 9137-9143.
18. Lin, Y.-P. and R.L. Valentine, *Reuctive Dissoltuion of Lead Dioxide (PbO2) in Acidic Bromide Solution.* Environmental Science and Technology, 2010: p. 3895-3900.

19. Liu, H., G.V. Korshin, and J.F. Ferguson, *Interactions of Pb (II)/Pb (IV) solid phases with chlorine and their effects on lead release.* Environmental Science & Technology, 2009. **43**(9): p. 3278-3284.

20. Ng, D.-Q., T.J. Strathmann, and Y.-P. Lin, *Role of Orthophosphate As a Corrosion Inhibitor in Chloraminated Solutions Containing Tetravalent Lead Corrosion Product PbO2.* Environmental Science & Technology, 2012. **46**(20): p. 11062-11069.

21. Xie, Y., Y. Wang, and D.E. Giammar, *Impact of chlorine disinfectants on dissolution of the lead corrosion product PbO2.* Environmental Science & Technology, 2010. **44**(18): p. 7082-7088.

22. Xie, Y., et al., *Effects of pH and carbonate concentration on dissolution rates of the lead corrosion product PbO2.* Environmental Science & Technology, 2010. **44**(3): p. 1093-1099.

23. Lin, Y.-P. and R.L. Valentine, *Reduction of lead oxide (PbO2) and release of Pb (II) in mixtures of natural organic matter, free chlorine and monochloramine.* Environmental Science & Technology, 2009. **43**(10): p. 3872-3877.

24. Lin, Y.-P. and Y. Zhang, *Determination of PbO2 Formation Kinetics from the Chlorination of Pb(II) Carbonate Solids via Direct PbO2 Measurement.* Environmental Science & Technology, 2011.

25. Liu, H., et al., *Formation of Pb (III) Intermediates in the Electrochemically Controlled Pb (II)/PbO2 System.* Environmental Science & Technology, 2012. **46**(3): p. 1430-1438.

26. Wang, Y., et al., *Kinetics of PbO2 Reductive Dissolution: Role of Pb (II) Adsorption and Surface Speciation.* Journal of colloid and interface science, 2012.

27. Liu, H., G.V. Korshin, and J.F. Ferguson, *Investigation of the kinetics and mechanisms of the oxidation of cerussite and hydrocerussite by chlorine.* Environmental Science & Technology, 2008. **42**(9): p. 3241-3247.

28. Noel, J. and D. Giammar. *The Influence of Water Chemistry on Dissolution Rates of Lead (II) Carbonate Solids Found in Water Distribution Systems.* in *Water Quality Technology Conference, Cincinnati, OH.* 2008.

29. Xie, Y. and D.E. Giammar, *Effects of flow and water chemistry on lead release rates from pipe scales.* Water Research, 2011. **45**(19): p. 6525-6534.

30. Noel, J.D., Y. Wang, and D.E. Giammar, *Effect of water chemistry on the dissolution rate of the lead corrosion product hydrocerussite.* Water research, 2014. **54**: p. 237-246.

31. Edwards, M., S. Jacobs, and D. Dodrill, *Desktop guidance for mitigating Pb and Cu corrosion by-products.* AWWA, 1999. **91**(5).

2 CHAPTER TWO: LITERATURE REVIEW

2.1 EXPOSURE TO LEAD

Lead is a toxic heavy metal found in the earth's crust. Due it its malleable nature, slight corrosion resistance, and low cost it has historically been used in almost every facet of society. It has been used in many consumer items (televisions, plastics, metal sheeting, automobiles etc.), acid batteries, gasoline, paint, pipes and solder [1]. Lead is ubiquitous, with exposure pathways ranging from air, soil, dust, paint, drinking water, and various consumer products.

Lead service lines in drinking water distribution systems, in addition to lead-bearing plumbing materials (e.g., leaded solder, brass fixtures), provide an important exposure pathway through drinking water [1]. Homes built before the mid-1980s are more likely to have lead service lines and lead-leaching plumbing materials within their water distribution network [1,2]. Many cities have implemented programs to replace the lead service lines running between municipal water mains and individual buildings in older districts. These replacement programs are extremely costly and progress very slowly. Drinking water service lines often cross between municipal land (sidewalks, roads etc.) and private land and so co-ordination with homeowners is required to facilitate a complete lead service line removal. If the homeowner does not replace the private portion of the service line, a combined service line containing lead will remain – this presents a continued lead exposure pathway for residents within their drinking water [3-6]. Even plumbing within new homes may still contain up to 8% lead due to the use of brass fixtures, chrome plated facets, and galvanized iron [7]. In the United States (U.S.) the maximum lead content in new plumbing was reduced to 0.25% in an amendment to the Safe Water Drinking Act in early 2011 [8]. Despite these new regulations and service line replacement programs, dissolved lead in drinking water distribution systems remains a serious concern. It is estimated

that currently over 50% of infant lead exposure comes from drinking water [9]. It is estimated that 50-75% of total lead at the tap is due to the presence of old lead service lines [10]. Despite widespread lead pipe replacement programs, there remains at least approximately 3.3 million lead service lines and 6.4 million lead service connections remaining in the mid-west and north-east of the United States alone [11].

2.2 CURRENT REGULATORY GUIDELINES

2.2.1 CANADA

The discovery of health concerns due to lead exposure brought about the introduction of several regulatory and non-regulatory initiatives to protect Canadian's safety. Many consumer items are now regulated by a combination of the Lead Risk Reduction Strategy for Consumer Products, Hazardous Products Act, Environmental Protection Act, or the Food and Drug Act [1,12]. Unfortunately the Canadian federal regulation for lead pipes and lead solder and drinking water exposure is more complex. The National Plumbing Code outlines the acceptable use of plumbing materials containing lead. This includes the highest allowable lead concentration within plumbing materials (i.e. in brass or chrome plating) as well as a ban on the use of lead solder [1].

The Health Canada Guidelines for Canadian Drinking Water Quality and Standards sets the limit for lead in drinking water for utilities at 10 µg/L. Health Canada (2009) provides two avenues for sampling protocol options (Table 2.1). Option 1 is a two tiered approach while option 2 has been presented for utilities that cannot meet the 6 hour stagnation time required by option 1 [13]. In the tiered approach, additional samples are only required (tier 2) if more than 10% of the samples taken in tier 1 are above the recommended action limit provided by Health Canada [13]. These guidelines, however, are not a federal regulation but a collaborative

suggestion from Health Canada and the Federal-Provincial-Territorial Committee [1]. The control of drinking water quality is a responsibility shared by both federal and provincial/territorial levels of government, however each jurisdiction is free to enact individual guidelines, objectives, and legislation (often based on the guideline).

TABLE 2.1: HEALTH CANADA (2009) RECOMMENDED SAMPLING PROCEDURES [13].

| | Option 1 | | Option 2 |
	Tier 1	Tier 2	
Stagnation Time	6 hr.	6 hr.	30 min.
Sample Type	1st Draw	1L Consecutive	1L Consecutive
No. samples/target	1	4	4
No. targets	population dependent	%10 of Tier 1 locations (minimum 2)	population dependent
Target Distribution	50% lead service line houses	---	50% lead service line houses
Escalate to Tier 2	If >10% samples are >15 ug/L	---	---

The Ontario Ministry of the Environment (MOE) has set a maximum acceptable concentration (MAC) of 10 µg/L for total dissolved lead standard [14]. The guidance document requires at least 2 samples per target location, and at least 1 target location per sampling event [15]. The MOE specifies a minimum 2 sampling events; one in the summer and one in the winter [15]. Similar to the Health Canada guidelines, the exact number of samples to be taken is population dependent and must include a mix of public and private buildings. The MOE recommended (but not required) stagnation time is 30 minutes followed by two 1 L samples [15].

Despite the outline of a recommended stagnation time and minimum sample requirements, the exact sampling procedure outlined by the document is vague [14]. Other information not specified by regulations are flush time, container type, analysis type, acid digestion time etc. A study that examined how stagnation times may affect dissolved lead concentrations in water samples collected at the tap found that a 5 minute flowing sample returned an average lead

concentration of 2.7 µg/L whereas a 6 hour stagnation yielded an average lead concentration of 3.5 µg/L [16]. Many utilities now use a combination of stagnation/first draw and multiple consecutive flowing sampling protocols to obtain total dissolved lead results. Strong evidence exists to support each sampling protocol under the basis of different research or sampling objectives [17].

2.2.2 UNITED STATES

Similarly to Canada, the U.S. has a collection of regulations protecting American's from lead exposure. The first initiative by the U.S. to control the use of lead in plumbing occurred as part of the 1986 'Federal Lead Ban' which amended the U.S. Safe Drinking Water Act [9]. This banned the use of solders and joins containing more than 0.2% lead which was a drastic reduction, as common older plumbing materials could have contained up to 50% lead [9].

To reduce lead service line corrosion the United States Environmental Protection Agency (U.S. EPA) issued the Lead and Copper Rule (LCR) under the Safe Drinking Water Act in 1991. This rule states that immediate action must be taken by the water utility to implement corrosion control strategies if 10% or more of the homes tested in the required yearly sampling meet or exceed a dissolved lead concentration of 15 µg/L. Currently, the LCR calls for a stagnation time of 6 hours and a first draw sample of 1L of cold water [18]. Recently, doubt has arisen to the effectiveness of the first draw sampling protocol mandated by the U.S. EPA [19]. Schock et al. (2014) discovered that dissolved lead rather than particulate lead was the primary cause for regulatory exceedances in distribution systems with lead corrosion control strategies in place [19]. In distribution systems where no corrosion control strategies had been employed, particulate lead was generally higher than dissolved lead. First draw samples do not necessarily represent both particulate and dissolved lead exposure [19]. To correct for this, Shock et al.

8

(2014) proposed a sampling protocol of a total of 30 1L samples across three flow rates to ensure samples are representative of concentrations in drinking water systems [19].

2.3 HEALTH EFFECTS OF LEAD IN DRINKING WATER

Lead is a toxic heavy metal and adversely affects human health with effects ranging from stomach distress to brain damage [20]. Until 2012, the Center for Disease Control (CDC) had set a 'blood level of concern' of 1 µg/L. Mounting evidence, however, has led to the CDC recently removing this limit and asserting that there is no safe blood level for children [21]. Above lead blood levels of 10 µg/L death and coma are a certainty; above 4 µg/L lead interferes with the production of red blood cells; above 2 µg/L lead is associated with nerve damage; above 1 µg/L lead has been associated with vitamin deficiencies and bone brittleness; and above 0.5 µg/L has been linked to an increased risk of miscarriage, early death from heart attacks or strokes, and high blood pressure [12]. Lead blood levels as low as 0.1 µg/L have been associated with many developmental deficiencies [12]. An examination of the Canadian census indicated that 2009 lead blood levels of Canadians ranged between 0.071 and 0.231 µg/L [22]. Since 2009, the known lead blood level of Canadians has not changed. There has been no studies done on the effects of lead in the bloodstream at such low levels, but there may be very subtle health effects [23]. Recent work has directly tied drinking water to elevated blood lead levels in children in the United States [24]. Children aged 6 and younger and pregnant women are especially at risk from exposure due to their ability to absorb lead because of the developing brain and body [9].

Children and adults absorb and react to lead very differently. It has been estimated that adults absorb approximately 3-15% of ingested lead while children can absorb as much as 50% [1]. This is due to children having a higher metabolic rate and an increased capacity to absorb any and all nutrients, including lead. Although immediate and acute effects of lead in the

body are most dangerous to pregnant women and children, anyone who has been exposed to lead can suffer lead toxicity. Absorbed lead can be stored in the bloodstream, soft tissues, and bones. However, when soft tissues or bones are stressed or damaged (due to age or acute trauma), up to 70% of the lead stored can be released back into the bloodstream and so acute toxicity can occur long after initial nominal ingestion [12]. Therefore lead represents a life-long risk to anyone, adult or child, who has been exposed to lead.

2.4 HISTORICAL EXCEEDANCES

In 2004 the Washington Post ran a story titled "Water in D.C. Exceeds EPA Lead Limit". This article revealed that over 4,000 homes throughout the city had elevated lead levels [25]. Analysis revealed that a switch in disinfectants from free chlorine to chloramines destabilized corrosion scale in lead pipes in the Washington DC water distribution system. The corrosion scale was predominately composed of lead (IV) oxides which had formed when free chlorine was used as the disinfectant prior to 2000. These lead (IV) oxides have a low solubility and so did not dissolve into the drinking water. In 2000, Washington D.C. switched disinfectant regimes; the switch from free chlorine to chloramines was intended to reduce disinfection by products (DBPs) that can occur when free chlorine and various organics interact [26]. Instead the change had the unintended consequence of lowering the oxidation reduction potential (ORP) of the distribution system. This led directly to the destabilization of lead (IV) oxides in the corrosion scale in the distribution system with higher lead dissolution rates resulting in high lead concentrations at the tap and lead toxicity within the population.

In light of the occurrence in Washington D.C., many municipalities around the world were forced to examine lead levels in their own drinking water systems. Currently, many major municipalities in Canada (e.g., Toronto, Ottawa, London, Montreal, Quebec City, and Vancouver

etc.) have reported elevated lead levels in drinking water and are in the process of implementing lead corrosion control strategies in addition to lead pipe replacement programs. Destabilization of the corrosion scale is complex and depends on numerous factors including pipe size and configuration, scale composition, water use patterns (stagnation times), and water chemistry [10]. Of these parameters, the only one that water utility operators can adjust to reduce lead levels at the point-of-use is water chemistry.

2.5 SCALE CHARACTERIZATION

Characterization of the solid phases present in the corrosion scale on the pipe interior is critical for developing effective corrosion control strategies. The composition of the corrosion scale depends strongly on the historical water chemistry that has flowed through the distribution system. There are many different types of lead compounds which can be present within the scale (Table 2.2). The most common lead (II) compounds found within drinking water systems are hydrocerussite, cerussite, and massicot/litharge, while the most common lead (IV) compounds are plattnerite/scrutinyite. Minium, a lead (II/IV) compound has also been observed [27]. High free chlorine concentrations (high ORP) generally results in the formation of lead (IV) oxides. A water composition of low ORP with moderate to high dissolved inorganic carbon (DIC) will often result in the formation of lead (II) carbonates as the main phase in the corrosion scale in lead service lines [28,29].

	Carbonate	Oxides	Other
Lead (II)	• $PbCO_3$ - Cerussite, • $Pb_3(CO_3)_2(OH)_2$ -Hydrocerussite, • Pb_2OCO_3, • $Pb_3O_2CO_3$, • $Pb_{10}(OH)_6O(CO_3)_6$	• PbO - Massicot or Litharge, • $Pb(OH)_2$, • $Pb_2O(OH)_2$	• PbS - Galena, • $PbCl_2$ - Cotunnite, • $PbCl_2$:$PbCO_3$ - Phosgenite, • $PbClF$ - Matlockite, • $PbOHCl$ - Laurionite, • PbI_2, • $PbSO_4$, • $Pb(NO_3)_2$, • etc.
Lead (IV)	• $Pb(CO_3)_2$	• PbO_2 - Plattnerite or Scrutinyite	
Lead (II/IV)		• Pb_3O_4 - Minium, • Pb_2O_3	

2.6 LEAD (IV) OXIDES

The primary lead (IV) oxide found in lead pipe corrosion scale is PbO_2. This lead (IV) oxide can be present as a polymorph of either plattnerite or scrutinyite. Plattnerite has a lower solubility than scrutinyite. If the conditions are favorable for the formation of PbO_2, plattnerite will develop first [30]. If lead (IV) oxides are the dominant phases in the scale, they will control the dissolved lead concentration over extremely long stagnation times (weeks to months) or if a reductant such as natural organic matter (NOM) is introduced into the distribution system. PbO_2 is very sensitive to changes in ORP of the bulk water within lead pipes, and so a switch between free chlorine and chloramines (lowering ORP) will dissolve PbO_2 into aqueous lead (II) carbonates or lead (II) ions. In turn, the lead (II) carbonates can also dissolve into the drinking water. In general, if a system has been exposed to free chlorine then it is likely safe to assume that some lead (IV) oxides exist within the distribution system [30].

A study of pipes across over 30 distribution systems operating with a range of chemistry conditions found that 26% of the systems had PbO_2 present within the scale [31]. Within these samples, very few were uniform PbO_2; most were a blend with lead (II) carbonates. This blended

scale of lead (IV) oxides and lead (II) carbonates was also found during a laboratory pipe loop study performed with very high chlorine concentrations (3.5 mg/L Cl_2) and high pHs (>9.5) [32]. The final scale within these laboratory pipes was a blend of lead (IV) oxides and lead (II) carbonates [32]. Both studies found that lead (II) carbonates played a significant role during the formation of the lead (IV) oxides and corrosion scales. Many studies have investigated the behavior of lead oxides under various drinking water conditions [30,32-51]. These include formation and dissolution studies, as well as the effects of NOM, ORP and disinfectant types, phosphates, iron, manganese, carbonate, and pH. Some of these studies also include lead (II) carbonates as they pertain to either the formation or dissolution of lead (IV) compounds [44-51].

2.7 LEAD CARBONATES

Lead (II) carbonates may control lead solubility in water distribution systems under flowing and short stagnation times. Specifically, cerussite and hydrocerussite are significantly more soluble than lead (IV) oxides. Extremely limited information exists about cerussite. The literature reported stability range of cerussite can vary widely [50,52]. In general it is thought that the stability of cerussite is within the range of a pH of 6 and 8; the exact limits of this range are uncertain [50,52-54]. Hydrocerussite is the stable form of lead (II) carbonates in a basic pH range (approximately 7 or 7.5 and higher) based on solubility and thermodynamic constraints [50]. If hydrocerussite reaches equilibrium in 1 hour (or less) and compliance monitoring requires stagnant time for up to 6 hours, then the lead concentrations in systems with lead (II) carbonates operating at pHs near or above neutral will most likely be controlled by solubility of hydrocerussite [49].

2.7.1 SCALE CHARACTERISTICS

Lead (II) carbonates can form in the presence of a high concentration of DIC and reducing conditions. Even under high oxidizing conditions (high ORP), lead (II) carbonates can still form in conjunction with lead (IV) oxides [32]. A study performed on corrosion scale samples harvested from the water distribution system in London Ontario found that hydrocerussite was the primary lead phase in 8 samples and cerussite was the primary scale in the remaining 3 samples [27]. Lead (IV) oxides were present, but were not the dominant phase. These results tend to be in agreement with corrosion scale characterization from other municipalities.

2.7.2 EQUILIBRIUM CONSTANTS FOR LEAD (II) CARBONATES

The dissolution of the lead (II) carbonates cerussite and hydrocerussite is represented by:

$$Pb_3(CO_3)_2(OH)_2 + 2H^+ = 3Pb^{+2} + 2CO_3^{-2} + 2H_2O \qquad \text{(Eq. 2.1)}$$

$$PbCO_3 = Pb^{+2} + CO_3^{-2} \qquad \text{(Eq. 2.2)}$$
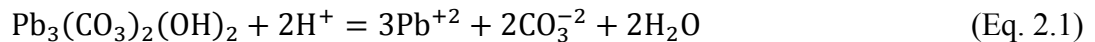
Equations 2.1 and 2.2 represent the equilibrium dissolution reactions of the most common lead (II) carbonates hydrocerussite and cerussite, respectively. Other chemical species within drinking water will also dictate total dissolved lead levels. A summary of these and their disassociation constants are presented in Table A.1 (Appendix 1, Supplementary Material). The reported equilibrium constants for lead solid phases are variable. A literature review found a large range in lead (II) carbonate experimentally derived equilibrium constants. The log solubility constants for hydrocerussite ranged from -18.861 to -14.322 and for cerussite ranged from -13.4 to -11.699 [52,55-60]. The literature sources are not mutually independent with some sources using similar base equilibrium constants (i.e. for water), and others injecting original work or calculations. All found equilibrium constants were standardized into the equation presented for hydrocerussite or

cerussite dissolution (Eq. 2.1 and 2.2) using reactions and known constants from Stumm et al. [57,60]. A pipe loop study performed by Edwards et al. estimated the equilibrium constants of both cerussite and hydrocerussite based on actual drinking water data to be -14.5 and -21.60, respectively [61]. This study also indicated that equilibrium models can over predict the actual dissolved drinking water concentrations by up to 10 times due to inaccurate or uncertain equilibrium constants. Future work was recommended on kinetics and temperature response of lead scales under realistic drinking water conditions rather than pursuing more accurate solubility products.

2.7.3   PREVIOUS MODELS ON LEAD COMPOUNDS

There are many models that have been developed to describe lead-aqueous interactions and contaminant intrusion into pipes, some of which date back to the 1980s [50,52,53,62-72]. These models can be divided into, computational diffusion models of lead pipes [62-64], statistical models based on field data analysis or pipe loops [65-67] and thermodynamic equilibrium models [50,52,53,71,72]. These models can provide valuable insight into the relationship between water chemistry, corrosion scale composition, and total dissolved lead levels. They can also be useful tools for assessing long term effectiveness of corrosion control strategies. Significant error can occur due to lack of information, poor initial model parameters, inaccurate equilibrium constants, or omitted kinetic data for dissolution models. Including hydrocerussite in a model can significantly complicate the system and can result in problems predicting total dissolved lead, pH, and DIC [50]. Little information exists on the reaction rates of hydrocerussite, but they are crucial for an accurate model calculations [50]. In addition to determining which scale composition to include for modelling, there is a question of equilibrium constants for each solid phase (and for each aqueous complex). This complicates the modelling

process further, as there is a wide variation in reported solubility and stability constants for lead compounds. The formation range of cerussite is of some doubt. Due to the uncertainty of solubility constants, it is estimated that cerussite is stable somewhere between a pH of 6 and 8 [50]. Some literature exists on the transformation of hydrocerussite to cerussite. This has been seen during chlorinated experiments, pipe loops, and batch experiments however these experiments were run at a pH of approximately 7.5 [46].

COMPUTATIONAL DIFFUSION MODELS

Models based on the collection of data, and solving for a potential computational or analytical solution may work as long as values are within the range of the collected data. Statistical models in particular require a large dataset in order to function accurately.

The model developed by Kuch et al. (1982) was a combination of computational diffusion and mass transfer equations and expanded on the statistical work of others in the mid-1980s to enable estimates of dissolved lead at the tap with regards to stagnant or flowing water regimes [65]. The computational diffusion model of Leer et al. (2001) found difficulty finding an analytical solution to calculate total dissolved lead under some conditions [66]. A simple lead loop computational diffusion model was set up to investigate the kinetics and equilibrium of lead precipitation was created by Tan et al. (2008) [69]. Another computational model focuses on contaminants other than lead, and was extended by the author to work for lead dissolution in drinking waters [67].

STATISTICAL MODELS

Clement et al. (2000) developed a statistical model based on field data to estimate public exposure to lead in drinking water based on the pH and alkalinities of the water. Based on the findings of their statistical analysis, a future model should be developed comprised of 3 classes

of water composition, characteristics of local plumbing systems, and consumer consumption behavior [62]. Eisnor et al. (2004) developed a model to investigate how residence time of a pipe and the presence of chlorine or chloramines affect lead compound dissolution [63]. More recently Hayes et al. (2009) developed a statistical model to evaluate the area and time based effect of lead sampling methodology on total dissolved lead levels [64].

THERMODYNAMIC MODELS

Thermodynamic and kinetic models can be used to simulate the chemical reactions controlling dissolved lead concentrations in a drinking water distribution system. Several thermodynamic equilibrium models to describe lead solubility were developed in the 1980s [50,52,71,72]. While these models were able to provide insight in the aqueous-solid phase interactions governing lead solubility, the equilibrium models developed were generally not able to predict experimental total dissolved lead concentrations. Hem and Durum (1973) evaluated the solubility of lead in surface waters with a pH range of 7.5 to 8.5, and in the presence of lead (II) carbonate phases and $Pb(OH)_2$. This study concluded that hydrocerussite, in particular, had a negligible effect on dissolved lead levels due to its limited solubility within this range of pHs [52]. Another similar study performed by Patterson et al. (1977) presented an equilibrium model which included only $Pb(OH)_2$ and cerussite. They compared model estimates to laboratory experiments conducted at various DICs and used an updated solubility constant value for $Pb(OH)_2$, however inconsistencies were still observed between simulated and experimental lead concentrations. These inconsistencies led Patterson et al. to conclude that hydrocerussite was important, and should be included in future models. Schock (1980) updated the Patterson model and showed that the theoretical solubility of the lead solid phases (cerussite, hydrocerussite, $Pb(OH)_2$) was strongly dependent on DIC and pH. The model developed by Schock was

17

compared to experiments performed at pH 7, 8 and DIC (3-30 mg C/L) and it was found that the model still significantly under predicted experimental lead concentrations [72]. This was attributed to model limitations (atmospheric CO_2) and high uncertainty of the equilibrium constants for hydrocerussite, cerussite, and $Pb(OH)_2$. More recently, Marani et al. (1995) simulated lead solubility for the application of the treatment of battery acid wastewater [53]. Lead precipitation experiments were conducted a wide range of pHs (3.9-11.3) and DICs (0-150 mg C/L) [53]. In basic conditions (pH>8) the model consistently over predicted the experimental results by 2-3 times [53]. At these conditions hydrocerussite was experimentally observed to be the dominant phase but their model predicted a different dominant lead solid phase. Their expectations were for the presence of $Pb(OH)_{2(s)}$ whereas the actual aged suspension was primarily hydrocerussite [53]. This was attributed to interference from atmosphere and uncertainty with regards to thermodynamic solubility constants [53]. A common theme among these thermodynamic equilibrium models is the pervading uncertainty in the equilibrium solubility constants and an understanding that hydrocerussite is an important dominant phase within drinking water systems. These models, however, are all based on equilibrium conditions. It is the goal of this work to expand upon previous research and allow for the inclusion of time based kinetic calculations of the dissolution of hydrocerussite.

2.7.4 Previous Lead (II) Carbonate Dissolution Studies

All carbonate solids are considered to be among the most rapidly soluble minerals [73]. Dissolution rates for carbonates tend to increase with decreasing pH, under acidic conditions [30]. A study performed by Pokrovsky et al. (2005) investigated the dissolution of other, non-lead, carbonate compounds in a batch reactor [73]. Dissolution rates were found to be on the

order of 10^{-4} mol/m^{2}h at acidic pHs [73]. Although not hydrocerussite, dissolution rates of other carbonate compounds can provide a good comparison for the studied lead (II) carbonate.

Despite the prevalence of lead (II) carbonates in the corrosion scale of water distribution systems, to our knowledge only three prior studies have evaluated the dissolution of hydrocerussite under varying water chemistry conditions. The first two studies investigated the dissolution rates of hydrocerussite within small (84 mL) continuously stirred tank reactors (CSTRs) loaded with 1 g/L hydrocerussite under varying water chemistry parameters with residence times of either 30 or 60 minutes [48,49]. The first study by Noel et al. (2008) found dissolution rates on the order of 10^{-8} mol/m^{2}min and showed variation in dissolution rates with respect to pH and DIC [48]. The follow up study by Noel et al. (2014) found a dissolution rate on the order of 10^{-9} mol/m^{2}min and showed the inhibition of this rate by orthophosphate [49]. Neither study provided a kinetic dissolution rate expression for hydrocerussite [48,49]. Although these studies provide valuable insight into hydrocerussite dissolution under varying conditions, it is not possible to capture the kinetic dissolution behavior with 30 min residence times.

A third study by Xie et al. (2011) focused on how the influence of flowing and stagnant conditions on lead dissolution from the interior of pipes under varying water chemistry parameters. The scales within the conditioned pipes unintentionally had hydrocerussite as a dominant solid species [32]. In general, the study found that under high DIC conditions (50 mg C/L), total dissolved lead concentrations could reach up to 0.04 mg/L under stagnation and 0.035 mg/L under flowing conditions [32]. Similarly, at high pHs (pH>10), stagnant and flowing dissolved lead concentrations reached 0.02 mg/L and 0.025 mg/L, respectively [32]. It should be noted, however, that at least 0.03 mg/L of the condition with flowing high pH was due to particulate lead and that equilibrium with the hydrocerussite dominant scales was not reached

19

during the experiment. Other conditions examined during this study including the influence of chlorine, chloramines, and phosphates [32].

2.8 CONCLUSION

Elevated lead levels in drinking water poses serious public health concerns. As of 2012, the CDC stated that there is no safe lead exposure level for children, rendering the problem of lead in drinking water a major issue for municipalities with lead bearing plumbing materials in the water distribution networks. Lead corrosion scales in distribution systems are often comprised of lead (II) carbonate and lead (IV) oxide solid phases. At short time scales and under flowing regimes, the lead (II) carbonate phases generally control the dissolved lead concentrations at the tap. Specifically within drinking water systems run at basic conditions and high DICs, the dominant solid phase is typically hydrocerussite [50]. Modeling of lead corrosion scale-aqueous phase interactions is complex. Thermodynamic models rely on inaccurate equilibrium solubility constants and these constants are often associated with a high degree of uncertainty. Additionally, the kinetics of dissolution of lead (II) carbonates at relevant time intervals in drinking water systems is virtually unknown. The objective of this thesis is to evaluate the rate of dissolution of hydrocerussite under varying pH and DIC conditions, and to develop a rate expression that can be incorporated into future kinetic based water chemistry models to calculate lead dissolution.

2.9 REFERENCES

1.   Health Canada. *Lead Information Package - Some Commonly Asked Questions About Lead and Human Health*. Environmental and Workplace Health 2014 2009-04-23 [cited 2014 September 2014]; Available from: www.hc-sc.gc.ca.

2.   Government of Canada. *Reduce your exposure to lead*. Environmental Health 2014 2012-11-16 September 2014]; Available from: http://healthycanadians.gc.ca/.

3.   Boyd, G.R., et al., *Effect of changing water quality on galvanic coupling.* AWWA, 2012. **104**(3): p. 45.

4.   Edwards, M.A., *Discussion: Effect of Changing Water Quality on Galvanic Coupling.* AWWA, 2012. **104**(12): p. 65-82.

5.   Triantafyllidou, S. and M. Edwards, *Galvanic corrosion after simulated small-scale partial lead service line replacements.* AWWA, 2011. **103**(9): p. 85.

6.   Wang, et al., *Impact of galvanic corrosion on lead release from aged lead service lines.* Water Research, 2012.

7.   Triantafyllidou, S. and M. Edwards, *Lead (Pb) in tap water and in blood: implications for lead exposure in the United States.* Critical Reviews in Environmental Science and Technology, 2012. **42**(13): p. 1297-1352.

8.   U.S. Congress, *Reduction of Lead in Drinking Water (S.3874)*. 2010.

9.   United States Environmental Protection Agency (U.S. EPA), *Integrated Science Assessment for Lead (Second External Review Draft)*. 2012: Washington, DC.

10.   Sandvig, A., et al., *Contribution of service line and plumbing fixtures to lead and copper rule compliance issues*. 2008: Awwa Research Foundation.

11.   American Water Works Association Research Foundation (AWWARF), *Distribution System Water Quality Changes Following Implementation of Corrosion Control Strategies.* American Water Works Association Research Foundation,, 2000.

12.   Canadian Environmental Health Atlas. *Environmental Contaminants: Lead*. Canadian Environmental Health Atlas: Understanding Our Environment is Key to Promoting Health and Preventing Disease 2014 2012 [cited 2014 September]; Available from: www.ehatlas.ca.

13.   Health Canada, *Guidance on Controlling Corrosion in Drinking Water Distribution Systems*. 2009.

14.   Ontario Ministry of the Environment (MOE), *Technical support document for Ontario drinking water standards, objectives and guidelines.* Ontario Ministry of the Environment, Ontario, 2003.

15.   Ontario Ministry of the Environment (MOE). *Safe Drinking Water Act, Ontario Regulation 170/03, Schedule 15.1*. 2014   September 5, 2014]; Available from: e-laws.gov.on.ca.

16.   Triantafyllidou, S., et al., *Lead (Pb) quantification in potable water samples: implications for regulatory compliance and assessment of human exposure.* Environmental monitoring and assessment, 2013. **185**(2): p. 1355-1365.

17.   Schock, M.R. and F.G. Lemieux, *Challenges in addressing variability of lead in domestic plumbing.* Water Science & Technology: Water Supply, 2010: p. 793-799.

18. United States Environmental Protection Agency (U.S. EPA), *Lead and Copper Rule Guidance Manual* in *Volume II: Corrosion Control Treatment*. 1992, U.S.EPA.

19. Schock, M.R., et al., *Importance of Pipe Deposits to Lead and Copper Rule Compliance (In Press)*. AWWA, 2014. **106**(7).

20. United States Environmental Protection Agency (U.S. EPA). *Lead in Drinking Water: Fact Sheet*. EPA 810-F-93-001 1993 June 24, 2009 June 30, 2014].

21. Brown, M.J. and S. Margolis, *Lead in drinking water and human blood lead levels in the United States*. 2012: US Department of Health and Human Services, Centers for Disease Control and Prevention.

22. Bushnik, T., *Lead and bisphenol A concentrations in the Canadian population*. 2010: Health Reports.

23. Environment Canada. *Levels of Exposure to Substances of Concern*. 2014 2014-06-11 [cited 2014 September]; Available from: http://www.ec.gc.ca/.

24. Triantafyllidou, S., et al., *Lead Particles in Potable Water.* Journal-American Water Works Association, 2007. **99**(6): p. 107-117.

25. Nakamura, D., *Water in DC Exceeds EPA Lead Limit*, in *The Washington Post Company*. 2004.

26. United States Environmental Protection Agency (U.S. EPA), *Elevated Lead in D.C. Drinking Water. A Study of Potential Causative Events, Final Summary Report.* 2007: Washington, DC.

27. Kim, E.J. and J.E. Herrera, *Characteristics of lead corrosion scales formed during drinking water distribution and their potential influence on the release of lead and other contaminants.* Environmental Science & Technology, 2010. **44**(16): p. 6054-6061.

28. Lytle, D.A. and M.R. Schock, *Formation of Pb (IV) oxides in chlorinated water.* AWWA, 2005. **97**(11): p. 102-114.

29. Lytle, D.A., C. White, and M.R. Schock, *Synthesis of lead pyrophosphate, Pb2P2O7, in water.* Microscopy and Microanalysis, 2008. **14**(4): p. 335-341.

30. Foundation), W.W.R., *Lead(IV) Oxide Formation and Stability in Drinking Water Distribution Systems* Y.X. Yin Wang, and Daniel E. Giammar Editor. 2012.

31. Peng, C.-Y., et al., *Characterization of elemental and structural composition of corrosion scales and deposits formed in drinking water distribution systems.* water research, 2010. **44**(15): p. 4570-4580.

32. Xie, Y. and D.E. Giammar, *Effects of flow and water chemistry on lead release rates from pipe scales.* Water Research, 2011. **45**(19): p. 6525-6534.

33. Cao, M., et al., *Selected-control synthesis of PbO2 and Pb3O4 single-crystalline nanorods.* Journal of the American Chemical Society, 2003. **125**(17): p. 4982-4983.

34. Lin, Y.-P., M.P. Washburn, and R.L. Valentine, *Reduction of lead oxide (PbO2) by iodide and formation of iodoform in the PbO2/I-/NOM system.* Environmental Science & Technology, 2008. **42**(8): p. 2919-2924.

35. Lin, Y.-P. and R.L. Valentine, *Release of Pb (II) from monochloramine-mediated reduction of lead oxide (PbO2).* Environmental Science & Technology, 2008. **42**(24): p. 9137-9143.

36. Lin, Y.-P. and R.L. Valentine, *Reuctive Dissoltuion of Lead Dioxide (PbO2) in Acidic Bromide Solution.* Environmental Science and Technology, 2010: p. 3895-3900.

37. Liu, H., G.V. Korshin, and J.F. Ferguson, *Interactions of Pb (II)/Pb (IV) solid phases with chlorine and their effects on lead release.* Environmental Science & Technology, 2009. **43**(9): p. 3278-3284.

38. Ng, D.-Q., T.J. Strathmann, and Y.-P. Lin, *Role of Orthophosphate As a Corrosion Inhibitor in Chloraminated Solutions Containing Tetravalent Lead Corrosion Product PbO2.* Environmental Science & Technology, 2012. **46**(20): p. 11062-11069.

39. Shi, Z. and A.T. Stone, *PbO2 (s, plattnerite) reductive dissolution by aqueous manganous and ferrous ions.* Environmental Science & Technology, 2009. **43**(10): p. 3596-3603.

40. Shi, Z. and A.T. Stone, *PbO2 (s, plattnerite) reductive dissolution by natural organic matter: Reductant and inhibitory subfractions.* Environmental Science & Technology, 2009. **43**(10): p. 3604-3611.

41. Wang, Y., J. Wu, and D.E. Giammar, *Kinetics of the Reductive Dissolution of Lead (IV) Oxide by Iodide.* Environmental Science & Technology, 2012. **46**(11): p. 5859-5866.

42. Xie, Y., Y. Wang, and D.E. Giammar, *Impact of chlorine disinfectants on dissolution of the lead corrosion product PbO2.* Environmental Science & Technology, 2010. **44**(18): p. 7082-7088.

43. Xie, Y., et al., *Effects of pH and carbonate concentration on dissolution rates of the lead corrosion product PbO2.* Environmental Science & Technology, 2010. **44**(3): p. 1093-1099.

44. Lin, Y.-P. and R.L. Valentine, *Reduction of lead oxide (PbO2) and release of Pb (II) in mixtures of natural organic matter, free chlorine and monochloramine.* Environmental Science & Technology, 2009. **43**(10): p. 3872-3877.

45. Lin, Y.-P. and Y. Zhang, *Determination of PbO2 Formation Kinetics from the Chlorination of Pb(II) Carbonate Solids via Direct PbO2 Measurement.* Environmental Science & Technology, 2011.

46. Liu, H., G.V. Korshin, and J.F. Ferguson, *Investigation of the kinetics and mechanisms of the oxidation of cerussite and hydrocerussite by chlorine.* Environmental Science & Technology, 2008. **42**(9): p. 3241-3247.

47. Liu, H., et al., *Formation of Pb (III) Intermediates in the Electrochemically Controlled Pb (II)/PbO2 System.* Environmental Science & Technology, 2012. **46**(3): p. 1430-1438.

48. Noel, J. and D. Giammar. *The Influence of Water Chemistry on Dissolution Rates of Lead (II) Carbonate Solids Found in Water Distribution Systems*. in *Water Quality Technology Conference, Cincinnati, OH*. 2008.

49. Noel, J.D., Y. Wang, and D.E. Giammar, *Effect of water chemistry on the dissolution rate of the lead corrosion product hydrocerussite.* Water research, 2014. **54**: p. 237-246.

50. Schock, M.R., *Response of lead solubility to dissolved carbonate in drinking water.* AWWA, 1980. **72**(12).

51. Wang, Y., et al., *Kinetics of PbO2 Reductive Dissolution: Role of Pb (II) Adsorption and Surface Speciation.* Journal of colloid and interface science, 2012.

52. Hem, J. and W. Durum, *Solubility and occurrence of lead in surface water.* 1973.

53. Marani, D., G. Macchi, and M. Pagano, *Lead precipitation in the presence of sulphate and carbonate: testing of thermodynamic predictions.* Water Research, 1995. **29**(4): p. 1085-1092.

54. Bissengaliyeva, M.R., et al., *The heat capacity and thermodynamic functions of cerussite.* The Journal of Chemical Thermodynamics, 2012. **47**: p. 197-202.

55. Yoder, C.H. and N.J. Flora, *Geochemical applications of the simple salt approximation to the lattice energies of complex materials.* American Mineralogist, 2005. **90**(2-3): p. 488-496.

56. Essington, M., J. Foss, and Y. Roh, *DIVISION S-9—SOIL MINERALOGY.* Soil Sci. Soc. Am. J, 2004. **68**: p. 979-993.

57. Robie, R.A. and B.S. Hemingway, *Thermodynamic properties of minerals and related substances at 298.15 K and 1 bar (10\^ 5 Pascals) pressure and at higher temperatures.* US Geol. Survey Bull., vol. 2131, p. 461-461 (1995). 1995. **2131**: p. 461-461.

58. Parkhurst, D.L. and C.A.J. Appelo, *Description of Input and Examples for PHREEQC Version 3—A Computer Program for Speciation, Batch-Reaction, One-Dimensional Transport, and Inverse Geochemical Calculations*, in *U.S. Geological Survey Techniques and Methods, book 6, chap. A43, 497 p., available at http://pubs.usgs.gov/tm/06/a43.* . United States Geological Survey (USGS) and United States Department of the Interior (USDI),.

59. Allison, J.D., D.S. Brown, and K.J. Novo-Gradac, *MINTEQA2/PRODEFA2 Version 4 - A geochemical assessment model for environmental systems*, O.o.R.a.D. Environmental Research Laboratory, Editor. 1991, United States Environmental Protection Agency (U.S. EPA): Athens, Georgia. p. 106.

60. Stumm, W. and J.J. Morgan, *Aquatic Chemistry. Chemical Equilibria and Rates in Natural Waters.* . 3rd. ed. 1996, New York: John Wiley & Sons Inc.

61. Edwards, M., S. Jacobs, and D. Dodrill, *Desktop guidance for mitigating Pb and Cu corrosion by-products.* AWWA, 1999. **91**(5).

62. Clement, M., R. Seux, and S. Rabarot, *A practical model for estimating total lead intake from drinking water.* Water Research, 2000. **34**(5): p. 1533-1542.

63. Eisnor, J.D. and G.A. Gagnon, *Impact of secondary disinfection on corrosion in a model water distribution system.* Aqua-Journal of Water Supply, 2004. **53**(7): p. 441-452.

64. Hayes, C.R., *Computational modelling to investigate the sampling of lead in drinking water.* Water Research, 2009. **43**(10): p. 2647-2656.

65. Kuch, A. and I. Wagner, *A mass transfer model to describe lead concentrations in drinking water.* Water Research, 1983. **17**(10): p. 1303-1307.

66. Leer, D.V.D., et al., *Modelling the diffusion of lead into drinking water.* Applied Mathematical Modelling, 2002. **26**(6): p. 681-699.

67. Mansour-Rezaei, S. and G. Naser. *Contaminant Intrusion in Water Distribution Systems: An Ingress Model*. in *World Environmental and Water Resources Congress 2012@ sCrossing Boundaries*. 2012.

68. Pierrard, J.-C., J. Rimbault, and M. Aplincourt, *Experimental study and modelling of lead solubility as a function of pH in mixtures of ground waters and cement waters.* Water Research, 2002. **36**(4): p. 879-890.

69. Tan, T., Y. Chen, and H. Chen, *Theoretical modeling and numerical simulation of the corrosion and precipitation in non-isothermal liquid lead alloy pipe/loop systems.* Heat and Mass Transfer, 2008. **44**(3): p. 355-366.

70.   Woosley, R.J. and F.J. Millero, *Pitzer model for the speciation of lead chloride and carbonate complexes in natural waters.* Marine Chemistry, 2013. **149**: p. 1-7.

71.   Patterson, J.W., H.E. Allen, and J.J. Scala, *Carbonate precipitation for heavy metals pollutants. Journal of the Water Pollution Control Federation.* 1977. **49**(12): p. 2397-2410.

72.   Patterson, J.W. and J.E. O'Brien, *Control of lead corrosion.* AWWA, 1979. **71**(5): p. 264-271.

73.   Pokrovsky, O.S., S.V. Golubev, and J. Schott, *Dissolution kinetics of calcite, dolomite and magnesite at 25 °C and 0 to 50 atm pCO2.* Chemical Geology, 2005. **217**(3-4): p. 239-255.

3 Chapter Three: Influence of Key Water Chemistry Parameters on the Kinetics of Pure Hydrocerussite (Pb$_3$(CO$_3$)$_2$(OH)$_2$) Dissolution

3.1 Introduction

Lead is a toxic heavy metal, and exposure can result in serious health effects. Many municipalities around the world still have lead service lines in their drinking water distribution systems. These lead service lines are often old and corrosion scales have formed on the interior of the pipe. Lead can be released from these corrosion scales in two forms: particulate and dissolved compounds. Service line replacements have been implemented in many affected municipalities, but replacement programs are costly and progress slowly and so municipalities must implement corrosion control strategies to reduce lead levels in drinking water at consumer point-of-use. Destabilization of the corrosion scale is complex and depends on numerous factors including length and diameter of pipe, water chemistry, scale composition, water use patterns, and hydraulic flow regimes [1]. Water chemistry is the most accessible parameter for water utility operators to control to reduce lead levels. For instance, parameters such as pH, alkalinity (or dissolved inorganic carbon; DIC), disinfectant type (i.e., free chlorine, chloramines), and additives (i.e. orthophosphate) can be adjusted to reduce or eliminate destabilization of corrosion scales in water service lines [2-10].

A comprehensive understanding of the composition of the corrosion scale within lead service pipes is required to predict dissolved lead concentrations at point-of-use and to develop effective corrosion control strategies. The two major groups of lead solid phases present in the scale in lead service lines are lead (IV) and lead (II) compounds. The primary lead (IV)

compounds are plattnerite (PbO_2), scrutinyite (PbO_2), and minium (Pb_3O_4); the most significant lead (II) carbonates include hydrocerussite ($Pb_3(CO_3)_2(OH)_2$) and cerussite ($PbCO_3$). Factors that dictate the composition of the corrosion scale are water use patterns, pipe network configuration, and water chemistry [1].

The key water chemistry parameters that affect the composition of corrosion scales and the potential destabilization of the scale in distribution systems include pH, DIC, and disinfectant type. Lead (II) carbonates are considerably more soluble than lead (IV) oxides and their dissolution kinetics are substantially faster. As a result, destabilization of lead (II) carbonate phases typically dictates dissolved lead levels at the tap. The dissolution of hydrocerussite and cerussite are given by:

$$Pb_3(CO_3)_2(OH)_2 + 2H^+ = 3Pb^{+2} + 2CO_3^{-2} + 2H_2O \qquad \text{(Eq. 3.1)}$$

$$PbCO_3 = Pb^{+2} + CO_3^{-2} \qquad \text{(Eq. 3.2)}$$
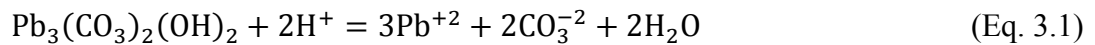
From these reactions it is clear that dissolution and formation of these solid phases will be a function of DIC and pH as well as a speciation of the dissolved lead within the solution. Additionally, the concentration of CO_3^{-2} will also change with respect to pH, resulting in complex relationships between the DIC, pH and solid phase solubility. Current United States Environmental Protection Agency (U.S. EPA) and Ontario Ministry of the Environment (MOE) guidelines recommend that water distribution systems maintain a pH between 6.5 and 8.5 and an alkalinity between 30 and 500 [11,12]. At a pH of 8, this corresponds to an approximate DIC range from 7.5 to 122 mg C/L. Experiments run within these limits will represent drinking water conditions. Based on thermodynamic constraints, hydrocerussite is generally the most stable form of lead (II) carbonates above a pH of 7 or 7.5 whereas cerussite is stable under more acidic conditions [13]. Previous studies have shown that lead (II) carbonates are generally the dominant

solid phase in distribution systems with excess DIC [14]. The dissolution of these phases is strongly influenced by alkalinity - or a combination of DIC and pH [9]. An increase of DIC concentrations generally stabilize the lead carbonate phases thereby reducing dissolved lead levels. In some cases the observed benefits of DIC addition can be limited, and there may be a maximum addition of DIC for optimal reduction of dissolved lead [15,16]. The type of disinfectant used by the water utility can also impact the composition of the corrosion scale as disinfectants directly affect the oxidation-reduction potential (ORP). Lead (II) carbonate phases can be transformed into less soluble lead (IV) phases under the highly oxidizing conditions caused by the use of free chlorine [9,14]. Alternatively, lead (IV) oxides can become destabilized when ORP is decreased by switching disinfectants (i.e., from free chlorine to chloramines). Destabilization due to lowered ORP has also been seen with the addition or increased concentration of other reducing species (i.e. dissolved natural organic matter (NOM), iodide, manganese, etc.) [17-23]. It is possible for lead (IV) oxides, as part of their dissolution process, to transform directly into lead (II) carbonates [9].

Several studies have conducted batch equilibrium experiments or developed thermodynamic equilibrium models to investigate the dissolution of lead solid phases present in corrosion scales [5,13,24-26]. These studies provide important insights into the influence of water chemistry parameters on corrosion scale dissolution and solid phase transformations. Equilibrium studies however do not accurately reflect dissolved lead levels within water distribution systems because the contact time between water and corrosion scale is typically not long enough for equilibrium conditions to be achieved. There is a need to investigate the kinetics of the dissolution processes under different water chemistry conditions to better approximate corrosion scale dissolution and soluble lead levels in water distribution systems.

Currently, the U.S. EPA lead and copper rule (LCR) testing protocol requires a pre-sample stagnation time of up to 6 hours for the first draw sample and any subsequent samples taken during flowing conditions [27]. The MOE legislation recommends a 30 minute stagnation time, with two consecutive 1L samples [28]. Previous work investigating hydrocerussite dissolution achieved stable equilibrium dissolved lead concentrations between 1 and 2 hours [29]. If hydrocerussite is the dominant phase in the corrosion scale, a combination of thermodynamic and kinetic dissolution rate will dictate dissolved lead at the point-of-use under U.S. EPA sampling protocols. Previous research on hydrocerussite dissolution kinetics is limited. Recent studies by Noel et al. [15,29] were the first to quantify hydrocerussite dissolution rates under typical conditions in water distribution systems. The experimental study used continuously stirred tank reactors (CSTRs) with residence times of 30 to 60 min. Since the dissolution of hydrocerussite may occur faster than 30 minutes, these residence times may be insufficient for kinetic rates determination. Additionally, a CSTR may not be the ideal experimental set up for the examination of fast dissolution reactions. Noel et al. reported an initial dissolution rate on the order of 10^{-8} to 10^{-9} mol/m^{2}min at pH values between 7 and 10 and DIC concentrations between 0 and 50 mg C/L [15,29]. In the absence of orthophosphate, the dissolution was strongly affected by pH and DIC [15,29]. Experimental steady state concentrations were reached in 1 hour or less. A rate expression to describe dissolved lead concentrations with respect to time was not derived [15,29]. They observed 2 stages in the hydrocerussite dissolution profiles: an initial stage with high variability with a potential peak in dissolved lead concentrations and a second stage of stable constant dissolution [15,29]. The potential peak identified in the first stage of dissolution may have been caused by an overloading

of the system with a high initial concentration of 1g/L. The work by Noel et al. has set the framework for the design of experiments within this study.

The objective of this work is to quantify the effects of pH and DIC on hydrocerussite dissolution kinetics and develop a rate expression to describe the dissolution rate and calculate dissolved lead under variable key water chemistry conditions. This was achieved by conducting batch dissolution experiments combined with numerical geochemical modeling in PHREEQC v.3.1.4 44

3.2 MATERIALS AND METHODS

3.2.1 MATERIALS

Hydrocerussite ($Pb_3(CO_3)_2(OH)_2$; Sigma-Aldrich) was used for all experiments without purification or modification. Sodium bicarbonate ($NaHCO_3$; Sigma-Aldrich, >99.5%) and sodium nitrate ($NaNO_3$; Sigma-Aldrich, >99.0%) were used to prepare a stock solution at the target DIC and at 0.01M ionic strength, respectively. Specific organic buffers were used depending on the target pH: EPPS (Alfa Aesar, 0.2 M, pH 8), CHES (Alfa Aesar, 0.5 M, pH 9), CAPSO (Alfa Aesar, 0.2 M, pH 9.5), and MOPSO (Alfa Aesar, 0.2 M, pH 7). For experiments conducted with chlorine, sodium hypochlorite ($NaOCl$; Fisher Scientific, 5.65-6% w/w, laboratory grade) was used as the free chlorine source to achieve a target concentration of 1 mg/L. Sodium hydroxide pellets ($NaOH$; Sigma-Aldrich) and concentrated nitric acid (HNO_3; EMD Milipore, Omnitrace, 67-70% v/v condensed) were used to prepare 0.1 M solutions. These solutions were then used to adjust the stock solution to the target pH (±0.05 pH units) immediately before each experiment started.

3.2.2 HYDROCERUSSITE DISSOLUTION EXPERIMENTS

Batch experiments were performed to quantify the dissolution of hydrocerussite. Batch experiments are recommended whenever possible to obtain homogeneous kinetic data [31]. Previous experiments performed by Noel et al. [15,29] used a CSTR. Often CSTR experiments are required to replicate conditions in distribution systems, in particular to maintain constant free chlorine levels. This was not required for our experiments as preliminary investigations found that chlorine does not impact short term (< 2 hours) hydrocerussite dissolution kinetics and so our batch experiments were performed in the absence of chlorine (Figure 3.6).

A summary of experiments conducted is presented in Table 3.1. To investigate the effect of pH on hydrocerussite dissolution, four experiments were run at different pH conditions where hydrocerussite is expected to be the dominant solid phase in the corrosion scale (pH 7.5, 8, 9, and 10; 20 mg C/L; Exp. 1-4). Competition and interference due to possible cerussite formation can occur at pHs lower than approximately 7.5 [13]. The effect of DIC was evaluated by conducting three experiments at DICs within the range of typical in drinking water distribution systems (10, 20, and 50 mg C/L; Exp. 1, 5-6) at a pH of 8. The influence of the initial hydrocerussite concentration was determined by conducting experiments with varying solid loading concentrations (10, 20, 50, and 1000 mg/L; Exp. 1, 7-9) at pH of 8 and a DIC of 20 mg C/L. Additional experiments were performed to quantify the effects of chlorine and organic buffers on the dissolution of hydrocerussite (Exp. 10-11). All experiments were run at an ionic strength of 0.01 M.

For the batch experiments, powder samples of solid hydrocerussite was weighed into 150 mL polypropylene bottles with the quantity based on the target solid loading. A pre-prepared stock solution was then added to each bottle. Stock solutions were prepared using NaHCO$_3$

powder and $NaNO_3$ powder measured into mega-pure water. If required, organic buffers (EPPS, CHES, CAPSO, or MOPSO) were used to buffer experiments at target pH values (Exp.1-9). These buffers have little to no known metal complexation and have been used in previous hydrocerussite dissolution studies [15,29,32]. Buffers were used to maintain the experimental pH at a known value to elucidate and isolate the effects of pH on hydrocerussite dissolution kinetics. An experiment performed without buffer showed that the addition of a buffer did not affect the dissolution results during the time frame of the experiment (Exp 10; Figure A.1; Appendix One, Supplementary Materials). At the start of the experiment, each bottle was half filled with stock solution and vigorously agitated to ensure the hydrocerussite powder was dispersed evenly. This ensured the hydrocerussite powder was not clumped together for the experiment, which would affect the results. The bottles were then filled completely (no headspace) and placed on a shaker table. This ensured that the batch experiments were run under closed conditions. The stock solution was not prepared under closed conditions, but alkalinity measurements were obtained to verify target DIC values. With the experimental procedure outlined, interference from atmospheric CO_2 is not expected [13].

Samples were obtained at set elapsed times after the stock solution was added. Each sample was taken from an individual bottle which was sacrificed after the sample was obtained. This ensured that experimental errors were not introduced due to changing mixing volumes, solid concentrations, preferential aqueous dispersion, or allowing the solution to be in contact with the atmosphere. Each sample was filtered through a 0.2 μm polyethersulfone filter using a 60 mL syringe – this prevented the dissolution reaction from progressing. Samples analyzed for total dissolved lead were acidified immediately using 2% HNO_3 and let rest in a cold room for at least 24 hours to ensure complete sample acid digestion. Samples for alkalinity were stored in 40 mL

polypropylene bottles with no headspace. Alkalinity, free chlorine, and pH measurements were obtained after filtering. All experiments were run in at least duplicate, with some individual points re-run at later dates to confirm that measurements were repeatable and to ensure the accuracy of sample and stock solution preparation procedures. As a result, some points have up to six sample results. Samples were taken at 2, 5, 10, 15, 20, 30, 45, 60, 90, and 120 minutes to capture hydrocerussite dissolution kinetics. Experimental times for equilibrium conditions to be reached depend on the water chemistry and initial hydrocerussite loading. The chosen sampling intervals were based on prior studies which had demonstrated that in basic conditions hydrocerussite typically reaches equilibrium in approximately 60 min [9,29]. Preliminary experiments performed indicated that appropriate kinetic data was obtained with these sampling intervals and all experiments reached equilibrium.

3.2.3 ANALYSIS METHODS

All samples were measured for total dissolved lead and alkalinity with some samples also tested for pH and total free chlorine. Dissolved lead measurements were determined by inductively coupled plasma optical emission spectroscopy (ICP-OES) using an average of the wavelengths 168.215 and 220.353. Experimental error associated with these wavelengths ranges from 0.03 to 0.06 mg/L [33]. Alkalinity measurements were taken on a metrohm auto titrator ($\pm$0.01 pH units). Measurements of pH were obtained using a Hanna Instruments HI 3222-01 benchtop meter with a sensitivity of $\pm$0.002. For the experiment conducted with chlorine (Exp. 11), free chlorine measurements were obtained by Hatch UV spectroscopy (UV-Vis) using method 8167 and powder pillows. This method has a sensitivity of $\pm$0.02 mg/L.

BET-N_2 analysis was performed in duplicate to characterize the specific surface area (SSA) of hydrocerussite used in the experiments. Specific surface area was determined to be

1.16 ± 0.02 m^2/g. Care was taken not to raise the temperatures above 120°C in this analysis, as this is known to cause degradation of hydrocerussite [34-38]. The specific surface area of the hydrocerussite used in this study was found to be lower than the value determined by Noel et al. [15,29] which was 4.8 m^2/g.

TABLE 3.1: SUMMARY OF EXPERIMENTAL CONDITIONS AND EXPERIMENTAL EQUILIBRIUM CONCENTRATIONS.

Experiment	Initial Hydrocerussite (mg/L)	pH (---)	DIC (mg C/L)	Chlorine (mg Cl$_2$/L)	Buffer (Y/N)	Experimental Equilibrium (total dissolved lead, mg/L)
1	10	8	20	0	Y	0.130 ± 0.0040
2	10	7.5	20	0	Y	0.202 ± 0.0059
3	10	9	20	0	Y	0.095 ± 0.0028
4	10	10	20	0	Y	0.163 ± 0.0048
5	10	8	10	0	Y	0.200 ± 0.0051
6	10	8	50	0	Y	0.094 ± 0.0040
7	20	8	20	0	Y	0.131 ± 0.0054
8	50	8	20	0	Y	0.125 ± 0.0041
9	1000	8	20	0	Y	---
10	10	8	20	0	N	---
11	10	8	20	1.2	N	---

3.2.4 EQUILIBRIUM MODEL

The geochemical modelling platform PHREEQC v.3.1.4 was used to simulate and interpret the experimental results [30]. PHREEQC is a commonly used program for calculation of a wide variety of aqueous systems. It relies on two ion association models, a Pitzer specific ion interaction model and the specific ion interaction theory aqueous model. PHREEQC can be used for speciation and saturation index calculations as well as batch reaction and one dimensional transport calculations. The model can include reversible or irreversible reactions including aqueous, mineral, gas, solid-solution, surface complexation, ion exchange equilibria, kinetic reactions, and pressure and temperature changes. In this work, PHREEQC was used to simulate the dissolution of hydrocerussite under various logKs for cerussite and hydrocerussite,

and to speciate a solution with a known total dissolved lead concentration. Reactions and associated equilibrium constants used in the model are presented in Table A.1 (Appendix One, Supplementary Materials).

To simulate the experiments the model was set up so that only hydrocerussite could dissolve, but both hydrocerussite and cerussite could precipitate. Lead (IV) oxides were not included in the model as only free chlorine present in Exp. 11 is capable of oxidizing lead (II) carbonates or aqueous lead (II) into lead (IV) oxides. Although several studies have reported equilibrium constants for hydrocerussite and cerussite, there is still considerable uncertainty associated with these values. Maximum and minimum values reported in literature are shown in Table 3.2 [24,30,39-43]. In some cases equilibrium constants were modified to be consistent with form of the hydrocerussite or cerussite dissolution reaction provided in Eqs.3.1 and 3.2 [41].

A study by Edwards et al. [16] investigated lead service line corrosion in actual drinking water systems. The majority of the scale present within the studied systems was comprised of hydrocerussite. This study found that models can over estimate dissolved lead levels in actual drinking water systems by up to 10 times due to the uncertainty in equilibrium constants [16]. Additionally, the study estimated the solubility products of hydrocerussite and cerussite using dissolved lead concentrations from drinking water systems and found both estimates were outside known literature values (Table 3.2) [16]. These values were obtained directly from literature, with the significant figures shown in Table 3.2 consistent with those presented in the original publications.

TABLE 3.2: RANGE OF LITERATURE REPORTED LOGK CONSTANTS FOR HYDROCERUSSITE AND CERUSSITE.

| | Literature Values | | Edwards (1999) [16] | PHREEQC Default Values [30] |
	Minimum	Maximum		
Hydrocerussite	-18.861	-14.322	-21.60	-18.7705
Cerussite	-13.4	-11.699	-14.5	-13.45

3.3 Experimental results and equilibrium model predictions

3.3.1 Influence of pH

Figure **3**.1 shows the dissolved lead concentrations as a function of time for the four experiments conducted at different pH values (Exps. 1-4). The results are consistent with prior studies that have shown that pH strongly controls the dissolution of lead (II) carbonates [13,44-47]. It can be seen that all experiments reached equilibrium between 40 and 60 minutes. The equilibrium for each pH experiment was determined as the average of the final stable end points (60 – 120 minutes), and is presented in Table 3.1. Equilibrium total dissolved lead concentrations were low for pH 8 and pH 9 (Exp. 1,3; Figure **3**.1) while the two experiments run at pHs closer to the edges of hydrocerussite's stability range (pH 7.5 and pH 10; Exp. 2,4) had higher equilibrium total dissolved lead concentrations.
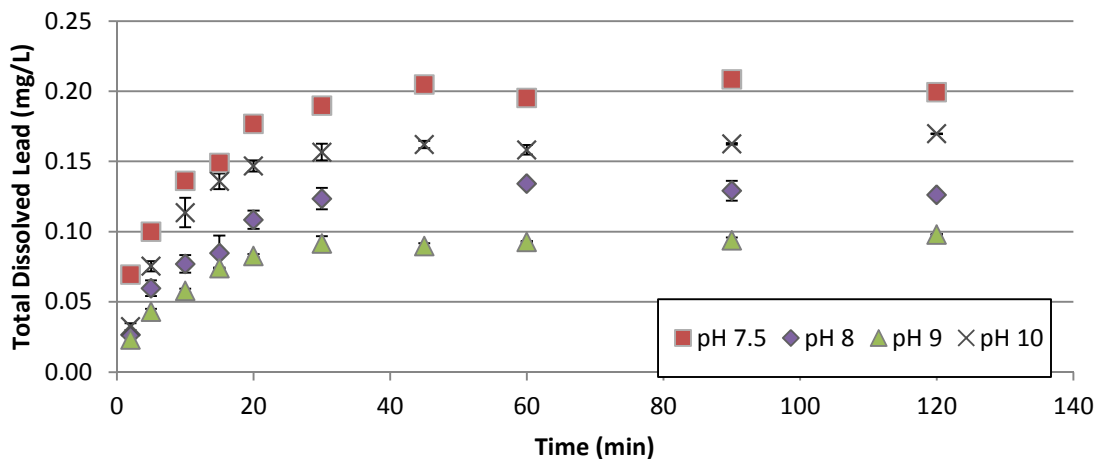

FIGURE 3.1: INFLUENCE OF PH ON TOTAL DISSOLVED LEAD FOR HYDROCERUSSITE DISSOLUTION EXPERIMENTS (EXP. 1-4; SOLID LOADING 10 MG/L, DIC 20 MG C/L, IS 0.01 M). ERROR BARS REPRESENT 1 STANDARD DEVIATION.

The equilibrium concentrations for the experiments run at different pH values were compared with model equilibrium estimates. The model was run using combinations of all the equilibrium constants previously reported for hydrocerussite and cerussite (Table 3.2) to provide

a maximum and minimum predicted equilibrium dissolved lead concentrations (Figure 3.2). It can be seen that the experimental results fall within the maximum and minimum limits of simulated total dissolved lead concentrations. Small changes in the hydrocerussite or cerussite equilibrium constants significantly affect the predicted dissolved lead level. The solubility product of cerussite significantly affected the upper limit of predicted dissolved lead, especially at pHs of 8 and lower. From the simulations it was found that the pH threshold, above which hydrocerussite is stable and below which cerussite is stable, varies between 7.5 and 8.5 depending on the specific equilibrium constants adopted. Therefore the results for the experiment performed at a pH of 7.5 (Exp. 2) may have been influenced by the formation of cerussite.

Due to the uncertainty associated with the equilibrium constants, experiments performed to investigate the effects of pH and DIC were used to estimate an equilibrium constant for hydrocerussite. For this, the experimental equilibrium total dissolved lead concentrations were speciated using PHREEQC under the experimental conditions (Table A.2; Appendix One: Supplementary Material). This provided values for Pb^{+2} and CO_3^{-2} for entry into an equilibrium expression for the dissolution reaction of hydrocerussite provided in Eq. 3.1 under experimental conditions. This was done using Exp. 1, and 3-8. Exp. 2 was neglected due to the possibility of cerussite interference. The average calculated log equilibrium constant was -15.98 ± 0.53 which fits within the range of literature values for hydrocerussite (Table 3.2).
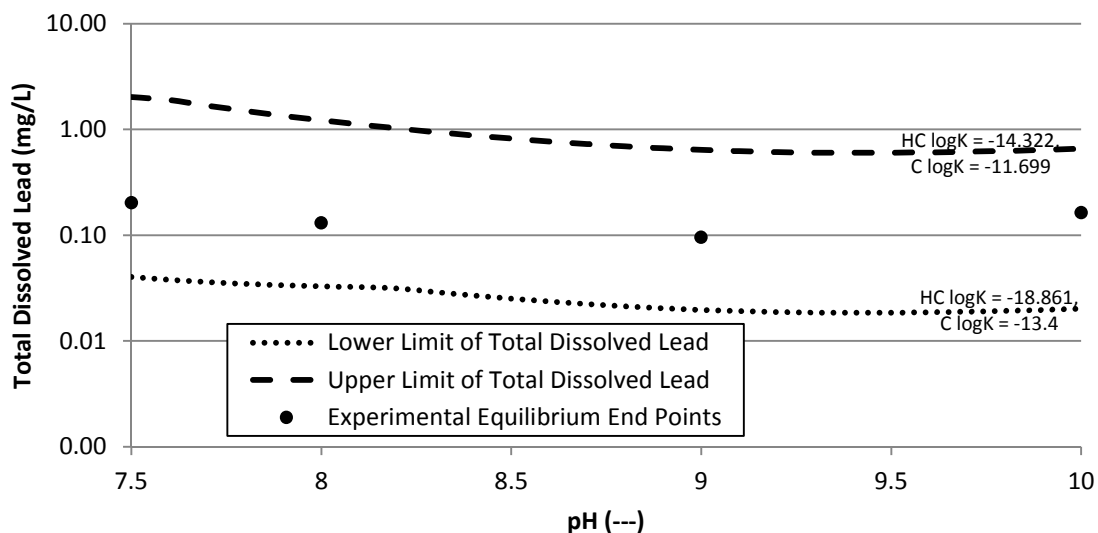
3.3.2 INFLUENCE OF DIC

The results of the three experiments conducted at different DIC concentrations (Exp. 1, 5, and 6) can be seen in Figure 3.3. Similar to the pH experiments, all DIC experiments reached equilibrium between 40 and 60 minutes and equilibrium concentrations were calculated by averaging the final stable concentrations between 60 and 120 minutes (Table 3.1). Consistent with prior studies, the DIC concentration considerably affected the final total dissolved lead concentrations [13,15,29,44-47]. The experiment with 10 mg C/L (Exp. 5) had the highest equilibrium total dissolved lead concentration, while 50 mg C/L (Exp. 8) had the lowest dissolved lead concentration. A low DIC typically results in a higher equilibrium total dissolved lead concentration, whereas a high DIC normally inhibits dissolution and lowers total dissolved lead concentrations [13]. The uncertainties of the equilibrium constants for cerussite and hydrocerussite also affect any model calculations for total dissolved lead with respect to DIC. Figure 3.4 shows a comparison between the maximum and minimum model predicted dissolved

lead range and the DIC experimental equilibrium results (Exp 1, 5, 6). As can be seen, the experimental values fit within the maximum and minimum ranges.

FIGURE 3.3: INFLUENCE OF DIC ON TOTAL DISSOLVED LEAD FOR HYDROCERUSSITE DISSOLUTION EXPERIMENTS (EXP. 1,5,6; SOLID LOADING 10 MG/L, PH 8, IS 0.01 M).
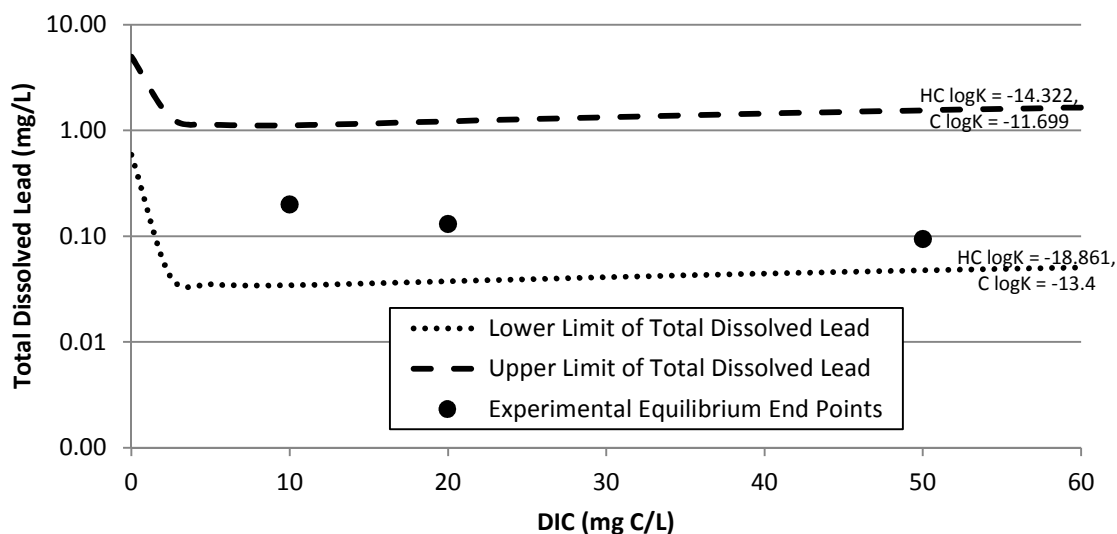
FIGURE 3.4: COMPARISON OF RANGE OF PREDICTED DISSOLVED LEAD VALUES AS A FUNCTION OF DIC WITH EXPERIMENTAL EQUILIBRIUM CONCENTRATIONS (EXP. 1,5,6; PH 8; IS 0.01M).

3.3.3 INFLUENCE OF INITIAL HYDROCERUSSITE SOLID LOADING

Previous dissolution experiments performed with solid lead compounds often used a solid loading of 1000 mg/L [9,15,29,47-52]. At this concentration, dissolution is very rapid and

equilibrium is reached too quickly for the measurement of dissolution kinetics. This was confirmed by a preliminary experiment that was run with a solid loading of 1000 mg/L (Exp. 9; Figure A.2; Appendix One, Supplementary Materials). At this initial concentration, equilibrium was not only achieved in less than 2 minutes, but there was an initial 'overshoot' in the measured dissolved lead concentration. Prior experimental studies have also observed this 'overshoot' behavior and it was generally attributed to either the dissolution reaction propagating faster than formation reactions or a rapid dissolution of very small particles within the initial solid sample [15,29,47,53].

An initial hydrocerussite concentration of 10 mg/L was found to be more suitable for obtaining kinetic data and this solid loading rate was used for all other experiments performed (Exp. 1-8, 10, 11). To ensure that this solid loading rate was realistic, preliminary calculations were performed to estimate the concentration of hydrocerussite in lead service lines. Specific surface areas (SSA) can differ significantly, with values in literature ranging from 0.812 - 4.8 m^2/g [9,15,29]. The hydrocerussite concentration was estimated to range from 25 and 185 mg/L assuming a pipe has an inner diameter of 1.9 cm with the interior surface covered smoothly in hydrocerussite with a SSA between 0.812 -4.8 m^2/g. Therefore the solid loading of 10 mg/L adopted for examining hydrocerussite dissolution in water distribution systems is realistic.

Total dissolved lead concentrations for experiments run with varying initial hydrocerussite solid loading are shown in Figure 3.5. Equilibrium concentrations were calculated by averaging over the final 60 to 120 minutes (Table 3.1). The experimental equilibrium total dissolved lead concentrations are independent of the initial hydrocerussite concentrations. This is expected, as hydrocerussite was available in excess for all experiments.

40

The variations between the equilibrium end points for these experiments fall within experimental error. It can be seen that equilibrium is achieved faster as the solid loading concentrations increases.
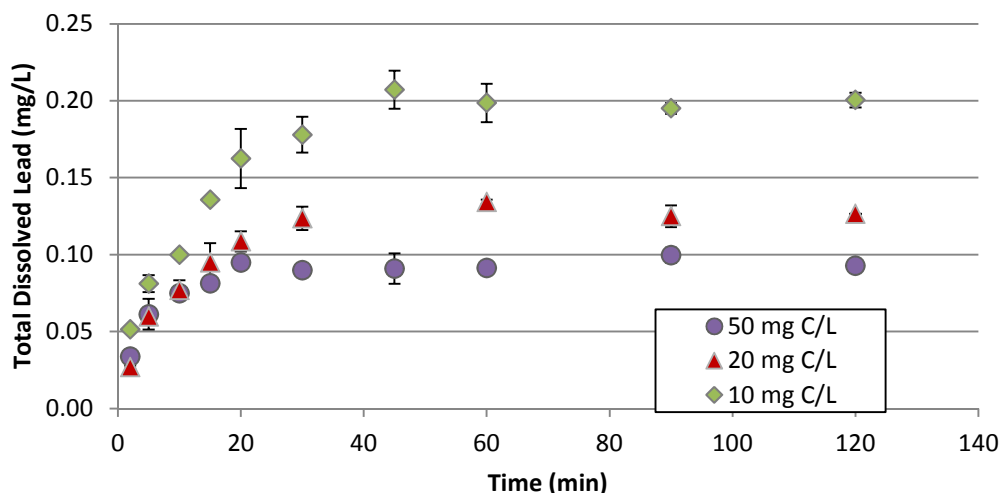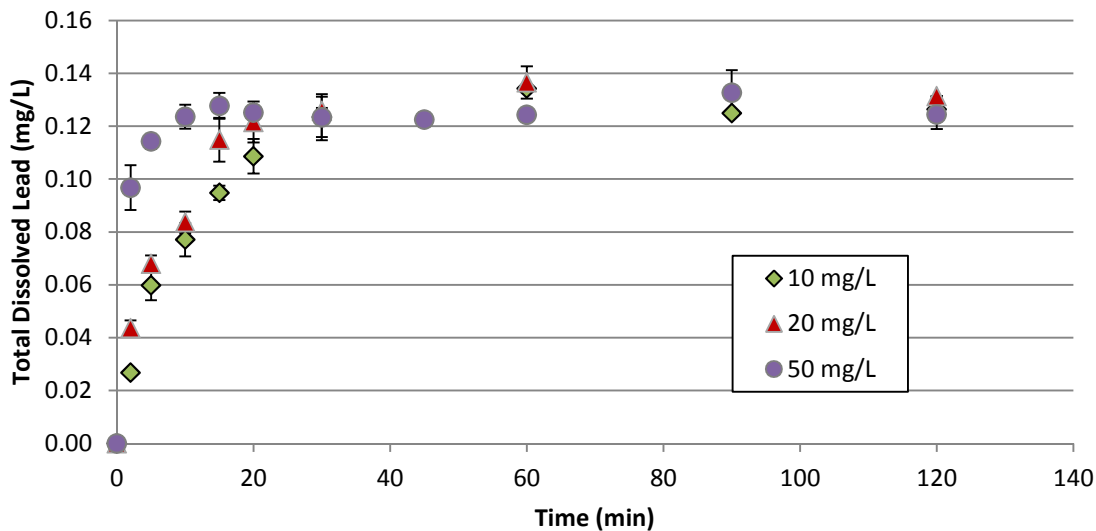

FIGURE 3.5: INFLUENCE OF SOLID LOADING ON TOTAL DISSOLVED LEAD FOR HYDROCERUSSITE DISSOLUTION EXPERIMENTS (EXP. 1,5,6; pH 8, DIC 20 MG C/L, IS 0.01 M).

3.3.4 INFLUENCE OF FREE CHLORINE

Prior studies indicate that chlorine may be able to oxidize the surface of hydrocerussite directly [9,51], which may affect the hydrocerussite dissolution kinetics. Experiments conducted with and without free chlorine (Exp. 11 and 1, respectively) revealed that chlorine does not affect short term hydrocerussite dissolution kinetics (Figure 3.6). The measured free chlorine concentrations through Exp. 11 are shown in Figure 3.6A, in addition to concentrations in the stock solution (not exposed to hydrocerussite). The experimental chlorine values were also normalized relative to the stock solution concentrations to clearly identify any chlorine consumption that may have occurred due to the presence of hydrocerussite. The stock solution was exposed to the same time scale, measurement errors, and experimental conditions as the experiments containing hydrocerussite to ensure that the values were comparable. The chlorine

41

was normalized by Eq. 3.3. Figure 3.6B shows that the chlorine did not degrade or react in the presence of hydrocerussite at the time scale of the experiments.

$$\text{Normalized Chlorine} = \frac{\text{Experimental Chlorine (mg Cl}_2\text{/L)}}{\text{Stock Solution Chlorine (mg Cl}_2\text{/2)}} \qquad \text{(Eq. 3.3)}$$
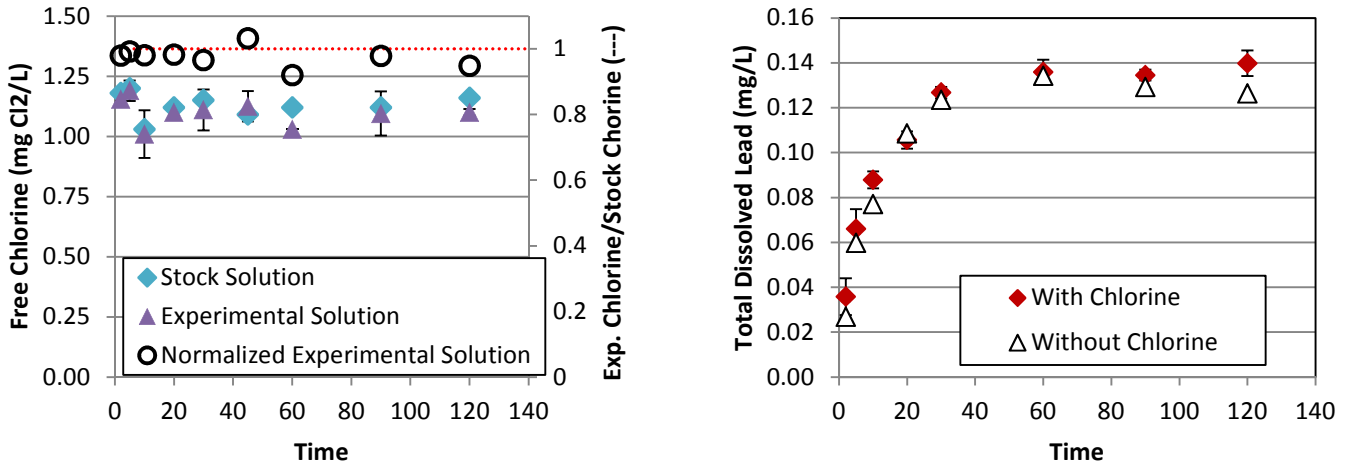
(a)   (b)

FIGURE 3.6: (A) MEASURED EXPERIMENTAL AND STOCK SOLUTION CHLORINE OVER TIME. DOTTED LINE REPRESENTS 1:1, OR NO CHANGE BETWEEN EXPERIMENTAL AND STOCK SOLUTIONS. (B) MEASURED TOTAL DISSOLVED LEAD OVER TIME FOR EXPERIMENT WITH CHLORINE (EXP. 11) AND WITHOUT CHLORINE (EXP. 1).

While previous studies have shown that chlorine, hydrocerussite, and total dissolved lead interact at longer time periods with chlorine transforming lead (II) carbonates or aqueous lead (II) into lead (IV) oxides [9], this reaction occurs on the scale of days and months rather than minutes [50]. Previous studies have reported lags in free chlorine reactions ranging from 2 hours up to almost 40 days [9,29,51]. Lui et al. (2008) quantified the influence of chlorine on hydrocerussite and cerussite stability and the subsequent formation of lead (IV) oxides over long stagnation times [9]. The length of this lag phase, but not necessarily the kinetic oxidation process, seemed to be influenced by pH, DIC, and chlorine concentrations [9]. During the lag phase Lui et al. (2008) observed an initial transformation from hydrocerussite to cerussite before eventual oxidation to lead (IV) oxides. These experiments, however, were conducted at a pH of 7 and

therefore the observed transformation could be attributed to the instability of hydrocerussite at lower pHs. While the effects of chlorine are extremely important for long term scale transformations, it was determined that chlorine does not influence hydrocerussite dissolution kinetics at the shorter time periods examined in this study.

3.4 DEVELOPMENT OF KINETIC EXPRESSION

An integral method of analysis was applied to determine a rate expression to describe the dissolution of hydrocerussite. Total dissolved lead concentrations were used to monitor the progress of the dissolution reaction. All rate expressions were determined using data from the first 20 to 30 minutes of each experiment. During this time period it was assumed that the hydrocerussite dissolution is the dominant reaction and that the rate of hydrocerussite formation is negligible. All dissolution curves were first normalized relative to equilibrium concentrations (Eq. 3.4).

$$\text{Normalized Concentrations} = N = \frac{C}{C_{(eq)}} = \frac{Pb^{+2}}{Pb_{(eq)}^{+2}} = \frac{Pb_T}{Pb_{T(eq)}} \qquad \text{(Eq. 3.4)}$$

Normalizing the data was important to compare the influence of different water chemistry conditions on the dissolution rates with no interference from equilibrium concentrations. It, in effect, translates the total dissolved lead concentrations into a measure of reaction progress (where the normalized concentration = 1 at equilibrium). Normalized concentrations can also be transformed into conversion factors which describe how far the experimental lead concentration is from experimental equilibrium conditions at any time. These are calculated by:

$$\text{Conversion Factor}(X_a) = 1 - N = 1 - \frac{C}{C_{(eq)}} = 1 - \frac{Pb^{+2}}{Pb_{(eq)}^{+2}} = 1 - \frac{Pb_T}{Pb_{T(eq)}} \qquad \text{(Eq. 3.5)}$$

Speciation calculations conducted using PHREEQC found that the conversion factors were the same irrespective of whether they were calculated based on aqueous Pb^{+2} or total dissolved lead

(Pb$_T$). This is because the percentage of Pb^{+2} in solution relative to Pb$_T$ remained constant over each experiment. To reduce speciation errors, all conversion factors were calculated using the measured total dissolved lead concentrations (Pb$_T$). If the dissolution of hydrocerussite follows a first order reaction rate, the expression describing the changing concentrations of dissolved lead in solution can be represented by Eq. 3.6a. Rearranging and combining Eq. 3.5 and 3.6a gives Eq. 3.6b which can be plotted to determine if the experimental results fit a first order expression:

$$C = C_{(eq)}(1 - e^{-kt}) \qquad \text{(Eq. 3.6a)}$$

$$-\ln(X_a) = kt \qquad \text{(Eq. 3.6b)}$$

3.4.1 INFLUENCE OF PH

To evaluate the influence of pH on dissolution rates, the dissolution curves for Exp. 1-4 were normalized based on their experimental equilibrium concentration (Eq. 3.4; Table 3.1). The original dissolution curves can be found in Figure **3**.1 and normalized curves in Figure 3.7. Further analysis transformed these curves into straight lines when graphed using Eq. 3.6b (Figure 3.8A).
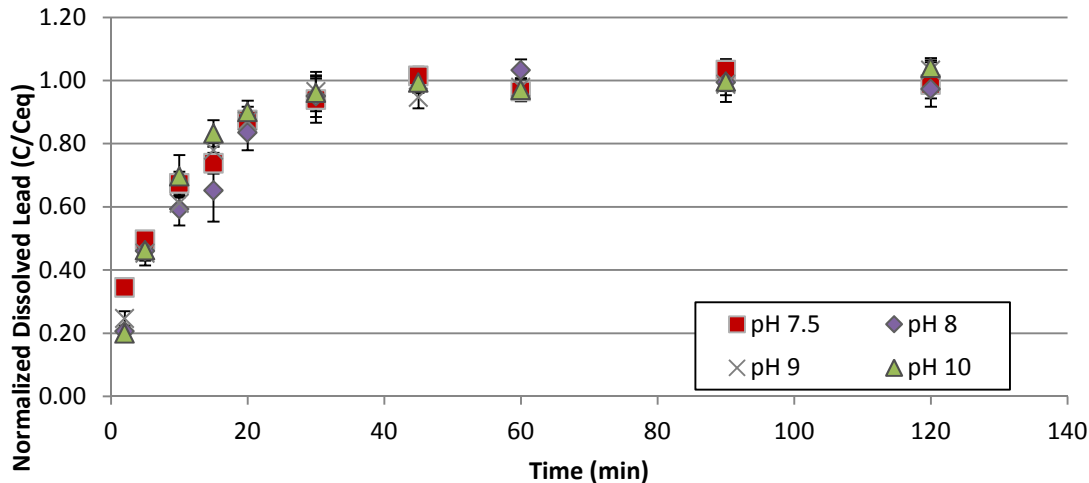

FIGURE 3.7: INFLUENCE OF PH ON NORMALIZED TOTAL DISSOLVED LEAD FOR HYDROCERUSSITE DISSOLUTION EXPERIMENTS (SOLID LOADING 10 MG/L, DIC 20 MG C/L, IS 0.01 M).
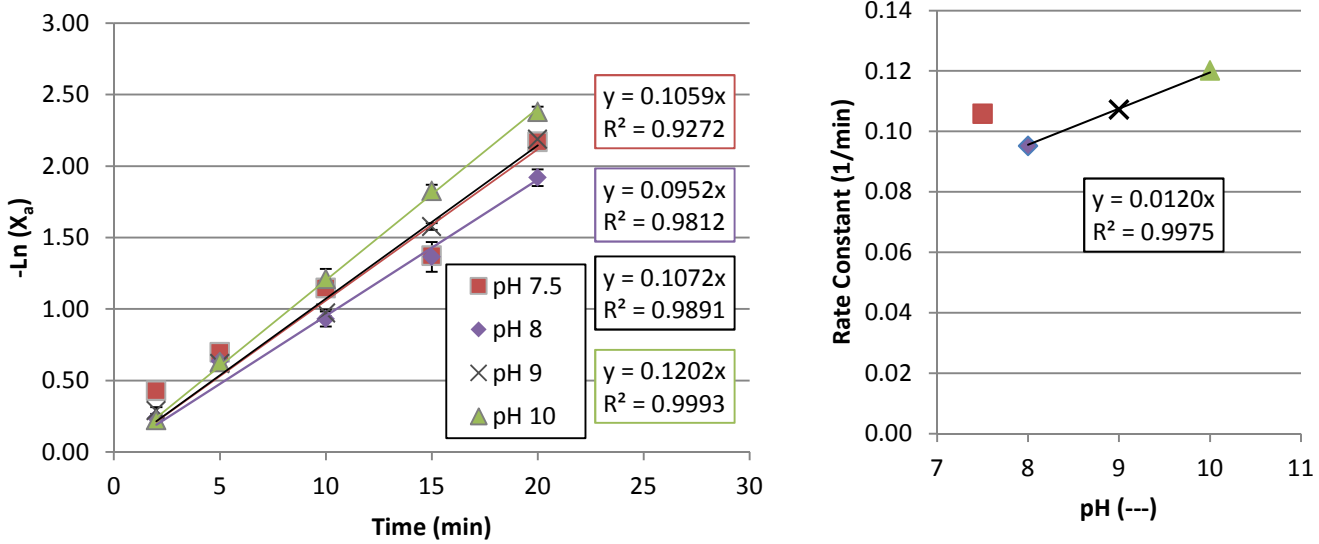
44

The linear relationships shown in Figure 3.8A indicate the dissolution within the first 20 minutes fits an irreversible first order dissolution expression (Eq. 3.6b). At the start of the experiment the reaction is far enough away from equilibrium to assume that any reverse reaction (i.e., hydrocerussite formation) is negligible. The rate constant determined for each pH experiment (Exp. 1-4) was plotted as a function of pH (Figure 3.8B). The rate constants determined for two experiments conducted at pH 7.5 and 8 (Exps. 1 and 2) were very similar, however at and above a pH of 8 the rate constant increased with increasing pH (Exp. 1, 3, and 4). The rate constant determined for pH 10 was the highest at 0.12 min^{-1}. It is thought that cerussite formation may have occurred in Exp. 2 (pH of 7.5) as the pH of this experiment is within the stability area of cerussite. This may have increased the rate constant. As a result the rate constant determined for Exp. 2 was not included in quantifying the relationship between the rate constants and pH. The rate expression with respect to pH was determined to be:

$$-\ln(X_a) = 0.0120 * (pH) * (t)$$

(Eq. 3.7)

The concentrations of individual species in solution through the experiments depend on pH, DIC, and total dissolved lead. The percentage composition of each individual species was found to be constant through each experiment because both pH and DIC are effectively constant. Figure 3.9 shows the four dominant aqueous species modelled to be present for each pH experiment – this speciation was determined using PHREEQC. As can be seen in Figure 3.9, the percentage of $Pb(CO_3)_2^{-2}$ increases significantly at higher pHs. At lower pHs, $PbCO_3$ is the dominant species. This shift in dominant aqueous species may contribute to the pH effects on hydrocerussite dissolution.
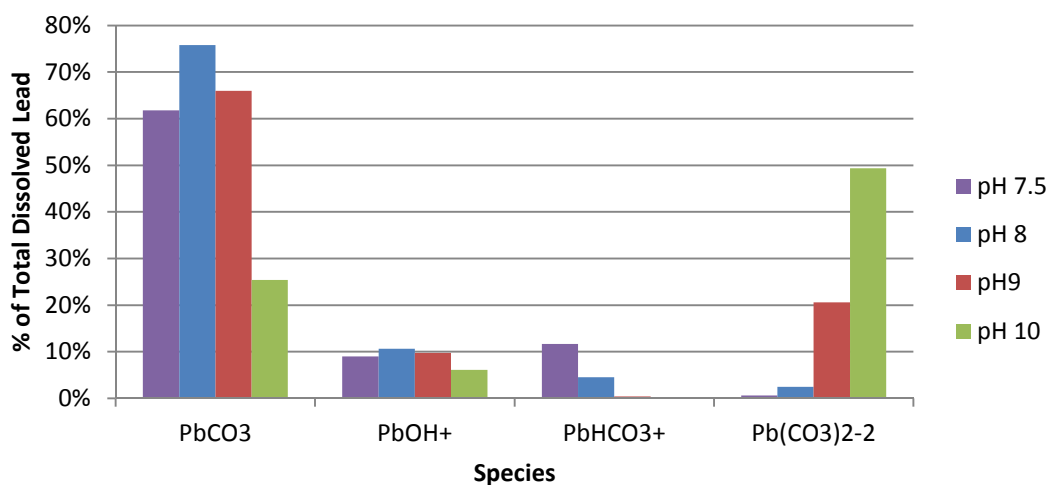
FIGURE 3.9: SIMULATED PERCENT SPECIES COMPOSITION FOR HYDROCERUSSITE DISSOLUTION EXPERIMENTS OF VARYING PHS (EXP. 1-4).

3.4.2 INFLUENCE OF DIC

Similar to analysis of the pH experiments, equilibrium values determined from the DIC experiments (Exp. 1, 5, 6; Table 3.1) were used to normalize the hydrocerussite dissolution curves (Eq. 3.4; Figure 3.10). The different normalized curves indicate that the DIC concentration influences the hydrocerussite dissolution kinetics. Each normalized dissolution curve was graphed to determine the rate constants (Figure 3.11A; Eq. 3.6b). The rate constant

was found to increase as DIC increases (Figure 3.11B). In fitting a linear relationship to Figure 3.11B, the rate constant was not forced through the origin since at 0 mg C/L a non-zero rate constant is possible. Possible relationships between the rate constants and individual carbonate species (e.g., H_2CO_3, HCO_3^-, and CO_3^{-2}) were also examined, however because the concentrations of these species are dependent on pH a linear relationship with DIC was chosen. The relationship found to describe the influence of DIC on the rate constant is:

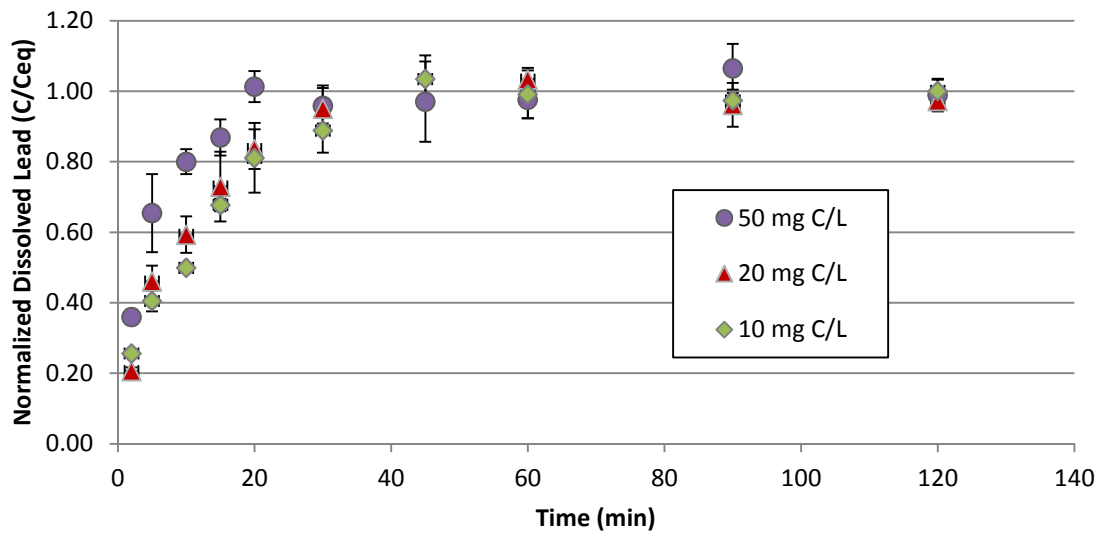$$-\ln(X_a) = (0.0018 * [DIC] + 0.0565) * (t) \qquad \text{(Eq. 3.8)}$$

FIGURE 3.10: INFLUENCE OF DIC ON NORMALIZED TOTAL DISSOLVED LEAD FOR HYDROCERUSSITE DISSOLUTION EXPERIMENTS (EXP. 1,5,6; SOLID LOADING 10 MG/L, PH 8, IS 0.01 M).
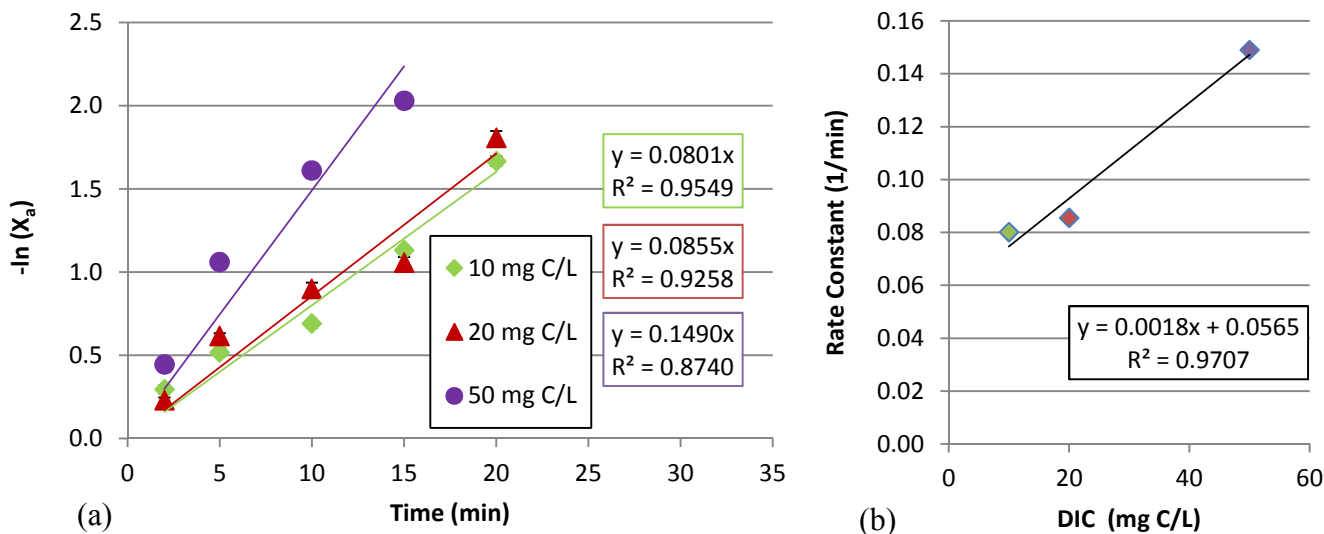
FIGURE 3.11: (A) DETERMINATION OF FIRST ORDER REACTION RATE FOR DIC EXPERIMENTS (EXP. 1,5,6) AND (B) FIRST ORDER RATE CONSTANTS AS A FUNCTION OF DIC.

Substituting a DIC of 20 mg C/L, as used in Exp.1, into Eq. 3.8, reduces the right hand side of the rate equation to 0.0997(t). This converges closely with Eq. 3.7 where the right hand side reduces to 0.096(t) for a pH of 8 (Exp. 1). Similar to the speciation performed for the pH experiments, the percent composition of individual species present remained constant through the individual DIC experiments over time. Figure 3.12 shows the simulated four dominant aqueous species in solution for each DIC experiment (Exp. 1,5,6). It can be seen that $PbCO_3$ is the dominant species for all three DIC dissolution experiments. As DIC increases, the percentage of $PbCO_3$ present in solution also increases - this is opposite to the trend found for the pH experiments. However, consistent with findings from pH experiments, as the percentage of $Pb(CO_3^2)^{-2}$ increases, the determined rate constant increases. This suggests that an increase in dissolution rate corresponds to a greater percentage of aqueous $Pb(CO_3^2)^{-2}$ present.
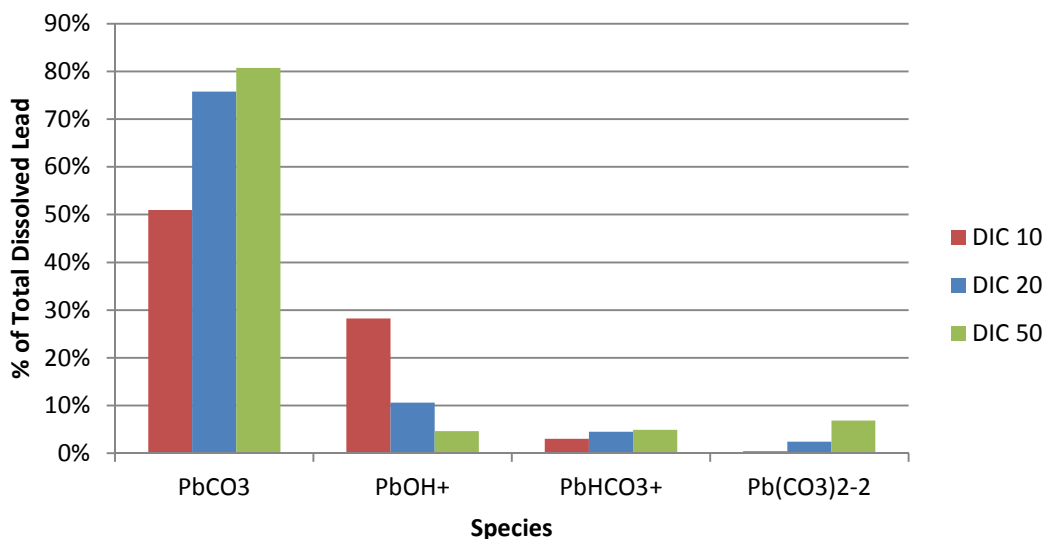
48

3.4.3 INFLUENCE OF HYDROCERUSSITE SOLID LOADING

Theoretically a change in the initial hydrocerussite concentration or solid loading should lead to a linear increase in the dissolution rate as the available surface area for reaction increases. Similar to pH and DIC, the solid loading dissolution curves were normalized relative to the experimental equilibrium concentrations (Figure 3.13). Although these experiments have the same equilibrium concentration, the experimental dissolved lead values were still normalized to directly compare the effects of solid loading on the dissolution rate relative to the influence of pH and DIC. As expected, when this data was analyzed using first order irreversible kinetics the lowest rate constant was found for the lowest solid loading of 10 mg/L and the highest rate constant was found for the highest solid loading (50 mg/L; Figure 3.14).
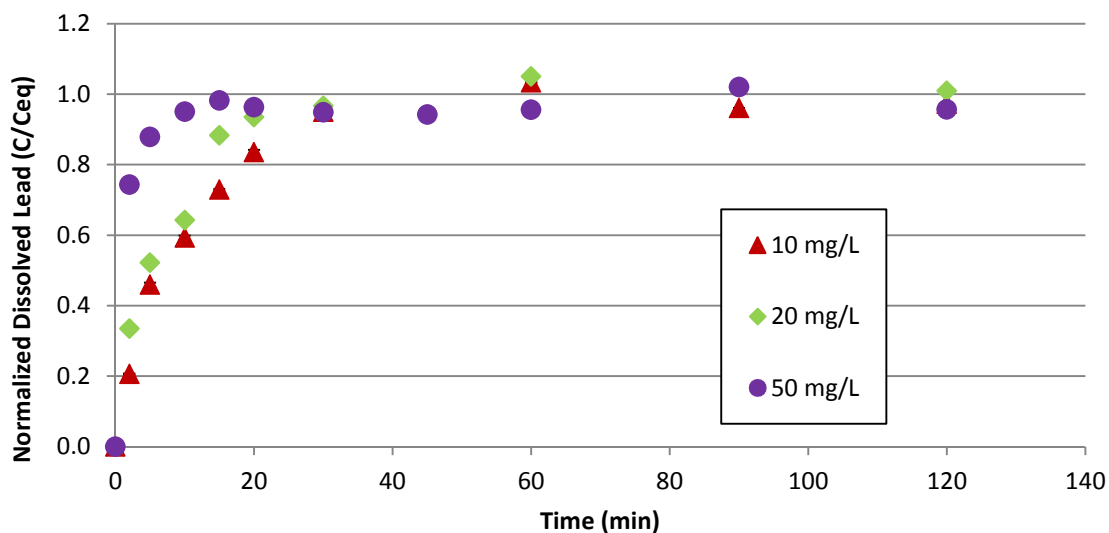
FIGURE 3.13: INFLUENCE OF SOLID LOADING ON NORMALIZED TOTAL DISSOLVED LEAD FOR HYDROCERUSSITE DISSOLUTION EXPERIMENTS (EXP. 1,7,8; pH 8, DIC 20 MG C/L, IS 0.01 M).
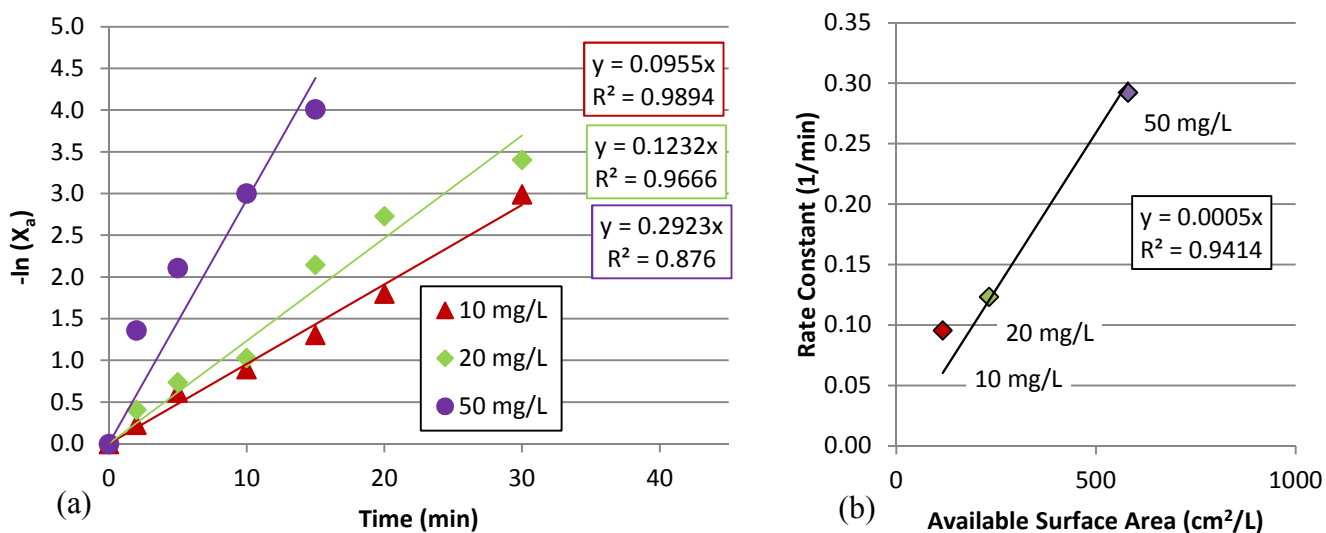
FIGURE 3.14: (A) DETERMINATION OF FIRST ORDER REACTION RATE FOR SOLID LOADING EXPERIMENTS (EXP. 1,7,8) AND (B) FIRST ORDER RATE CONSTANTS AS A FUNCTION OF SOLID LOADING.

To quantify the effect of the solid loading, the rate constants determined from Figure 3.14A were plotted against the available surface area. The N$_2$-BET analysis performed to

characterize the hydrocerussite determined a specific surface area (SSA) of 11.6 cm^2/g. The solid loading concentrations were converted to available surface area by:

$$\text{Available Surface Area} \left(\tfrac{\text{cm}^2}{\text{L}}\right) = \left[\text{Hydrocerussite} \left(\tfrac{\text{mg}}{\text{L}}\right)\right]_o * \text{SSA} \left(\tfrac{\text{cm}^2}{\text{L}}\right) \qquad \text{(Eq. 3.9)}$$

The variation between the fitted linear relationship and experimental rate constant at the lower solid loading rate (10 mg/L) in Figure 3.14B is thought to be due to clumping or incomplete dispersion of hydrocerussite particles at the initiation of the experiment. Using this linear relationship, an expression to describe the effect of solid loading on the dissolution rate was derived:

$$-\ln(X_a) = 0.0005 * [\text{Hydrocerussite}]_o * (\text{SSA}) * (\text{time}_{\text{min}}) \qquad \text{(Eq. 3.10)}$$

For the conditions used in Exp. 1 (solid loading of 10 mg/L), Eq. 3.10 results in a slightly lower value (0.058(t)) than either the pH or DIC rate expressions (3.9 and 3.10, respectively).

3.4.4 COMBINED EXPRESSION

An overall expression was developed to describe the combined effects of pH, DIC, and solid loading concentration on the hydrocerussite dissolution rate. This combined kinetic expression for hydrocerussite is valid over the experimental conditions examined in this study. The individual dissolution expression with respect to pH and solid loading (Eq. 3.7, 3.8, and 3.10) were combined to give:

$$-\ln(X_a) = (1.9 \times 10^{-6} * [\text{DIC}] + 6.5 \times 10^{-5}) * [\text{pH}] * [\text{Solid}] * (\text{SSA}) * (\text{time}_{\text{min}}) \quad \text{(Eq. 3.11)}$$

If Equation 3.11 is expanded, it can be seen that there are two parts to the combined equation. The first part incorporates the effects of changing pH, DIC, and solid loading concentrations. The second part only incorporates pH and solid loading, and represents the dissolution rate at a DIC of 0 mg C/L.

3.4.5 COMPARISON OF KINETIC MODEL WITH EXPERIMENTAL RESULTS

To test the combined dissolution expression (Eq. 3.11), estimates for total dissolved lead for the different pH, DIC and solid loading conditions were compared to the experimental results. This comparison can be seen in Figure 3.15. The normalized concentrations were chosen for comparison due to a continued uncertainty in the equilibrium constant for hydrocerussite. It can be seen that the combined rate expression provides an excellent match with the experimental dissolution curves the studied conditions.
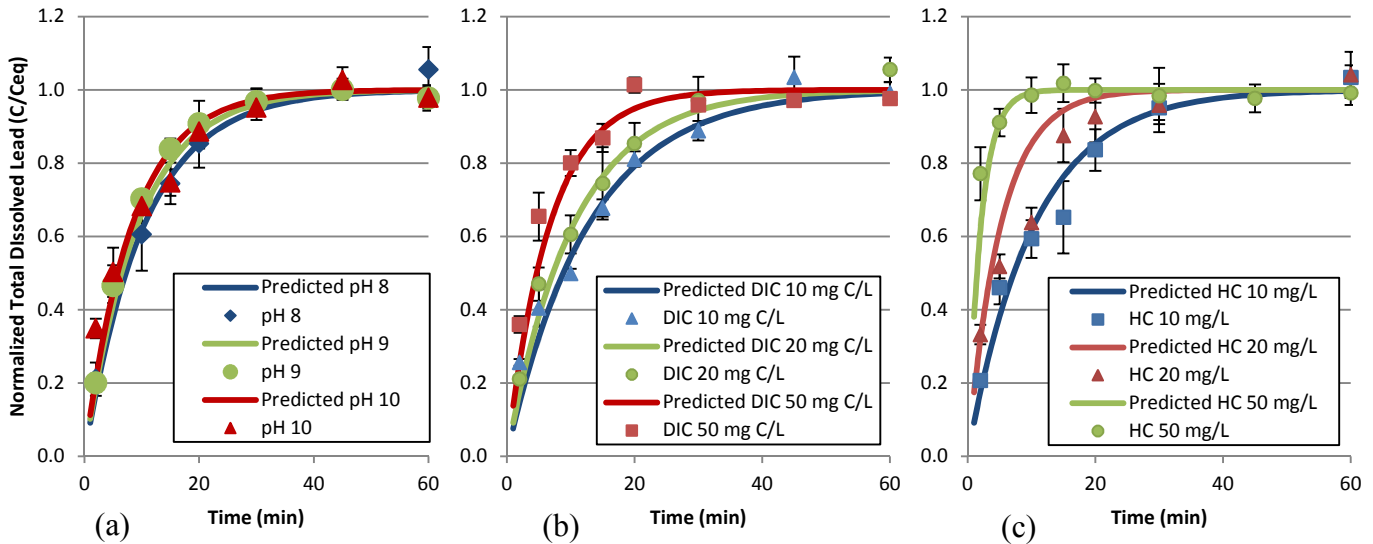
FIGURE 3.15: COMPARISON OF NORMALIZED EXPERIMENTAL AND ESTIMATED TOTAL DISSOLVED LEAD; (A) PH COMPARISON (EXP. 1-4), (B) DIC COMPARISON (EXP. 1,5,6), AND (C) SOLID LOADING COMPARISON (EXP. 1,7,8).

3.5 CONCLUSIONS AND FUTURE WORK

An estimated equilibrium solubility constant determined from experiments in this work was found to be -15.98 ± 0.53 which is within the limits of literature values. The effects of pH and DIC on equilibrium dissolved lead levels were consistent with previous studies. Dissolved lead concentrations were found to be lowest around a pH 9 with concentrations increases towards the bounds of the hydrocerussite stability region (pH 7.5 and 10). It was found that increasing

DIC decreased equilibrium total dissolved lead concentrations. As expected, the hydrocerussite solid loading had no effect on final equilibrium total dissolved lead concentrations. For all experiments, equilibrium was reached within 40 minutes, confirming that hydrocerussite dissolves very rapidly. A chlorine concentration of approximately 1 mg/L did not affect the dissolution of hydrocerussite at this time scale. This indicates that the oxidation of lead by chlorine occurs at longer durations than the experimental period explored in this study. While the dissolution rate constant was found to be inversely related to DIC values, it was found to increase as pH increased. This indicates that high DIC stabilizes hydrocerussite as well as lowering the equilibrium total dissolved lead concentrations. It is recommended that additional experiments are conducted to explore a wider range of DIC values including a DIC of 0. High solid loading rates and thus available solid surface area corresponded to higher hydrocerussite dissolution rates. This work also confirmed that concentrations of hydrocerussite of 1000 mg/L, are often used in lead solid phase dissolution studies, result in rapid dissolution and equilibrium conditions achieved in under 2 minutes. All expressions developed for pH, DIC, and solid loading converged within reasonable error to provide a combined rate expression that can be used to estimate the kinetic dissolution of lead for the water chemistry conditions considered. The results of this work provide a fundamental basis for further development of a kinetic based lead scale dissolution model.

3.6 REFERENCES

1. Sandvig, A., et al., *Contribution of service line and plumbing fixtures to lead and copper rule compliance issues*. 2008: Awwa Research Foundation.
2. Edwards, M., M.R. Schock, and T.E. Meyer, *Alkalinity, pH, and copper corrosion by-product release.* AWWA, 1996. **88**(3): p. 81-94.
3. Boyd, G.R., et al., *Effects of changing disinfectants on lead and copper release.* AWWA, 2008. **100**(11): p. 75-87.
4. Lin, N.-H., et al., *Lead corrosion control from lead, copper-lead solder, and brass coupons in drinking water employing free and combined chlorine.* Journal of Environmental Science & Health Part A, 1997. **32**(4): p. 865-884.
5. Marani, D., G. Macchi, and M. Pagano, *Lead precipitation in the presence of sulphate and carbonate: testing of thermodynamic predictions.* Water Research, 1995. **29**(4): p. 1085-1092.
6. Gouider, M., et al., *Impact of orthophosphate addition on biofilm development in drinking water distribution systems.* Journal of hazardous materials, 2009. **167**(1): p. 1198-1202.
7. Tam, Y. and P. Elefsiniotis, *Corrosion control in water supply systems: Effect of pH, alkalinity, and orthophosphate on lead and copper leaching from brass plumbing.* Journal of Environmental Science & Health Part A, 2009. **44**(12): p. 1251-1260.
8. Cantor, A.F., et al., *Effect of chlorine on corrosion in drinking water systems.* AWWA, 2003. **95**(5): p. 112-123.
9. Liu, H., G.V. Korshin, and J.F. Ferguson, *Investigation of the kinetics and mechanisms of the oxidation of cerussite and hydrocerussite by chlorine.* Environmental Science & Technology, 2008. **42**(9): p. 3241-3247.
10. Vasquez, F.A., *The Effect of free chlorine and chloramines on lead release in a distribution system*. 2005, University of Central Florida Orlando, Florida.
11. United States Environmental Protection Agency (U.S. EPA), *Integrated Science Assessment for Lead (Second External Review Draft)*. 2012: Washington, DC.
12. Ontario Ministry of the Environment (MOE), *Technical support document for Ontario drinking water standards, objectives and guidelines.* Ontario Ministry of the Environment, Ontario, 2003.
13. Schock, M.R., *Response of lead solubility to dissolved carbonate in drinking water.* AWWA, 1980. **72**(12).
14. Kim, E.J. and J.E. Herrera, *Characteristics of lead corrosion scales formed during drinking water distribution and their potential influence on the release of lead and other contaminants.* Environmental Science & Technology, 2010. **44**(16): p. 6054-6061.
15. Noel, J. and D. Giammar. *The Influence of Water Chemistry on Dissolution Rates of Lead (II) Carbonate Solids Found in Water Distribution Systems*. in *Water Quality Technology Conference, Cincinnati, OH*. 2008.
16. Edwards, M., S. Jacobs, and D. Dodrill, *Desktop guidance for mitigating Pb and Cu corrosion by-products.* AWWA, 1999. **91**(5).

17. Lin, Y.-P. and R.L. Valentine, *The release of lead from the reduction of lead oxide (PbO2) by natural organic matter.* Environmental Science & Technology, 2008. **42**(3): p. 760-765.

18. Lin, Y.-P. and R.L. Valentine, *Reduction of lead oxide (PbO2) and release of Pb (II) in mixtures of natural organic matter, free chlorine and monochloramine.* Environmental Science & Technology, 2009. **43**(10): p. 3872-3877.

19. Lin, Y.-P. and R.L. Valentine, *Release of Pb (II) from monochloramine-mediated reduction of lead oxide (PbO2).* Environmental Science & Technology, 2008. **42**(24): p. 9137-9143.

20. Lin, Y.-P. and R.L. Valentine, *Reuctive Dissoltuion of Lead Dioxide (PbO2) in Acidic Bromide Solution.* Environmental Science and Technology, 2010: p. 3895-3900.

21. Lin, Y.-P., M.P. Washburn, and R.L. Valentine, *Reduction of lead oxide (PbO2) by iodide and formation of iodoform in the PbO2/I-/NOM system.* Environmental Science & Technology, 2008. **42**(8): p. 2919-2924.

22. Shi, Z. and A.T. Stone, *PbO2 (s, plattnerite) reductive dissolution by aqueous manganous and ferrous ions.* Environmental Science & Technology, 2009. **43**(10): p. 3596-3603.

23. Shi, Z. and A.T. Stone, *PbO2 (s, plattnerite) reductive dissolution by natural organic matter: Reductant and inhibitory subfractions.* Environmental Science & Technology, 2009. **43**(10): p. 3604-3611.

24. Hem, J. and W. Durum, *Solubility and occurrence of lead in surface water.* 1973.

25. Patterson, J.W., H.E. Allen, and J.J. Scala, *Carbonate precipitation for heavy metals pollutants. Journal of the Water Pollution Control Federation.* 1977. **49**(12): p. 2397-2410.

26. Patterson, J.W. and J.E. O'Brien, *Control of lead corrosion.* AWWA, 1979. **71**(5): p. 264-271.

27. United States Environmental Protection Agency (U.S. EPA), *Lead and Copper Rule Guidance Manual* in *Volume II: Corrosion Control Treatment*. 1992, U.S.EPA.

28. Ontario Ministry of the Environment (MOE). *Safe Drinking Water Act, Ontario Regulation 170/03, Schedule 15.1*. 2014   September 5, 2014]; Available from: e-laws.gov.on.ca.

29. Noel, J.D., Y. Wang, and D.E. Giammar, *Effect of water chemistry on the dissolution rate of the lead corrosion product hydrocerussite.* Water research, 2014. **54**: p. 237-246.

30. Parkhurst, D.L. and C.A.J. Appelo, *Description of Input and Examples for PHREEQC Version 3—A Computer Program for Speciation, Batch-Reaction, One-Dimensional Transport, and Inverse Geochemical Calculations*, in *U.S. Geological Survey Techniques and Methods, book 6, chap. A43, 497 p., available at http://pubs.usgs.gov/tm/06/a43.* . United States Geological Survey (USGS) and United States Department of the Interior (USDI),.

31. Missen, R.W., Mims, C.A., Saville, B.A., *Introduction to Chemical Reaction Engineering and Kinetics*. 1999, New York: John Wiley & Sons.

32. Aplichem, *Biological Buffers*. 2008.

33. Ventures, I. *Inorganic Standards & Custom Reference Materials*. Periodic Table 2014 [cited 2014; Available from: http://www.inorganicventures.com/periodic-table.

34. Ball, M. and M. Casson, *Thermal studies of lead (II) salts, VI.* Journal of Thermal Analysis and Calorimetry, 1983. **28**(2): p. 371-380.

35.	Beck, C., *Differential Thermal Analysis Curves of Carbonate Minerals.* ?, ?

36.	Flemming, N.J., et al., *Thermal decomposition of basic lead carbonates: a comparison of hydrocerussite and plumbonacrite.* Thermochimica Acta, 1984. **81**: p. 1-8.

37.	Zivkovic, Z.D., *Kinetics and mechanism of thermal decomposition of lead carbonate.* Journal of Thermal Analysis and Calorimetry, 1979. **16**(1): p. 3-11.

38.	Zivkovic, Z.D. and B. Dobovivsek, *Determination of reaction kinetics based on a part of a differential thermal analysis or thermogravimetric curve.* Thermochimica Acta, 1979. **32**(1): p. 205-211.

39.	Yoder, C.H. and N.J. Flora, *Geochemical applications of the simple salt approximation to the lattice energies of complex materials.* American Mineralogist, 2005. **90**(2-3): p. 488-496.

40.	Essington, M., J. Foss, and Y. Roh, *DIVISION S-9—SOIL MINERALOGY.* Soil Sci. Soc. Am. J, 2004. **68**: p. 979-993.

41.	Robie, R.A. and B.S. Hemingway, *Thermodynamic properties of minerals and related substances at 298.15 K and 1 bar (10\^ 5 Pascals) pressure and at higher temperatures.* US Geol. Survey Bull., vol. 2131, p. 461-461 (1995). 1995. **2131**: p. 461-461.

42.	Allison, J.D., D.S. Brown, and K.J. Novo-Gradac, *MINTEQA2/PRODEFA2 Version 4 - A geochemical assessment model for environmental systems*, O.o.R.a.D. Environmental Research Laboratory, Editor. 1991, United States Environmental Protection Agency (U.S. EPA): Athens, Georgia. p. 106.

43.	Stumm, W. and J.J. Morgan, *Aquatic Chemistry. Chemical Equilibria and Rates in Natural Waters.* . 3rd. ed. 1996, New York: John Wiley & Sons Inc.

44.	Grimes, S.M., S.R. Johnston, and D.N. Batchelder, *Lead carbonate-phosphate system: solid-dilute solution exchange reactions in aqueous systems.* Analyst, 1995. **120**(11): p. 2741-2746.

45.	Schock, M. and M. Gardels, *Pumbodolvency reduction by high pH and low carbonate - solubility relationships.* AWWA, 1983. **75**(1): p. 88 - 91.

46.	Todd, G. and E. Parry, *Character of lead hydroxide and basic lead carbonate.* 1964.

47.	Xie, Y., et al., *Effects of pH and carbonate concentration on dissolution rates of the lead corrosion product PbO2.* Environmental Science & Technology, 2010. **44**(3): p. 1093-1099.

48.	Wang, Y., J. Wu, and D.E. Giammar, *Kinetics of the Reductive Dissolution of Lead (IV) Oxide by Iodide.* Environmental Science & Technology, 2012. **46**(11): p. 5859-5866.

49.	Xie, L. and D.E. Giammar, *Equilibrium solubility and dissolution rate of the lead phosphate chloropyromorphite.* Environmental Science & Technology, 2007. **41**(23): p. 8050-8055.

50.	Xie, Y., Y. Wang, and D.E. Giammar, *Impact of chlorine disinfectants on dissolution of the lead corrosion product PbO2.* Environmental Science & Technology, 2010. **44**(18): p. 7082-7088.

51.	Liu, H., G.V. Korshin, and J.F. Ferguson, *Interactions of Pb (II)/Pb (IV) solid phases with chlorine and their effects on lead release.* Environmental Science & Technology, 2009. **43**(9): p. 3278-3284.

52.	Liu, H., et al., *Formation of Pb (III) Intermediates in the Electrochemically Controlled Pb (II)/PbO2 System.* Environmental Science & Technology, 2012. **46**(3): p. 1430-1438.

53. Wang, Y., et al., *Kinetics of PbO2 Reductive Dissolution: Role of Pb (II) Adsorption and Surface Speciation.* Journal of colloid and interface science, 2012.

4 CHAPTER FOUR: CONCLUSIONS AND RECOMMENDATIONS

4.1 CONCLUSIONS

Batch dissolution experiments were performed on the pure lead (II) carbonate phase hydrocerussite under a short time interval (<2 hr.). These experiments were conducted at four pHs (7.5, 8, 9, and 10), three DIC values (10, 20, and 50 mg C/L), and three solid loading concentrations (10, 20, and 50 mg/L). The experimental conditions examined were chosen to represent a broad range of drinking water conditions under which hydrocerussite could be exposed. Additional experimental conditions were performed to explore the impact of buffering the experiments, chlorinated conditions (approximately 1 mg Cl_2/L), and high solid loading rates (1000 mg/L). These experiments revealed that the addition of buffer or chlorine to the experimental solution did not affect the dissolution of hydrocerussite at the time scale studied (<2 hr.). High solid loading rates resulted in equilibrium conditions been reached in less than two minutes.

All experiments achieved equilibrium conditions within 40 minutes which confirms that hydrocerussite dissolution occurs rapidly. The measured equilibrium total dissolved lead was low for pH 8 and pH 9 while the two experiments run at pHs closer to the edges of hydrocerussite's stability range (pH 7.5 and pH 10) had higher concentrations. At a pH of 7.5 the dissolution reaction may have been affected by cerussite formation because this pH is close to the transition pH between cerussite and hydrocerussite (cerussite is the dominant phase at low pHs; hydrocerussite at high pHs). The exact stability ranges of these lead (II) carbonates are uncertain. In general, equilibrium concentrations increased with decreasing DIC, supporting the fact that the addition of DIC suppresses lead dissolution. As expected, the initial concentration of

58

hydrocerussite did not affect equilibrium concentrations. All experimental equilibrium concentrations were within the range of minimum and maximum limits predicted by the geochemical modelling software PHREEQC based on literature sourced solubility constants. Equilibrium concentrations from experiments were used to determine an approximate solubility product for hydrocerussite of -15.98 ± 0.53 which is within the range found in literature.

An integral method of analysis was used to evaluate how the rate constant of the dissolution reaction changes under various pH, DIC, and solid loading conditions. When evaluated, all experimental total dissolved lead curves resulted in a straight line confirming that this reaction follows a first order dissolution rate. Kinetic rate expressions were first developed for each of the three conditions studied. In general, it was found that the rate constant increased with increasing pH, DIC, and solid loading rates. Additionally, experimental total dissolved lead values were speciated using PHREEQC to identify any trends within the aqueous lead species with respect to changing rate constant. The aqueous species $Pb(CO_3)_2^{-2}$ was found to increase with increasing rates. The individual rate equations for the 3 conditions converged within reasonable error, indicating that they are different parts of the same expression. These expressions were combined into one overall expression which incorporated the effects of total dissolved lead, DIC, pH, initial hydrocerussite concentration, and specific surface area. This expression matched well when compared with the original experimental dissolution curves. The derived rate expression for hydrocerussite can be used to estimate the kinetic dissolution of this lead (II) carbonate to total dissolved lead under the range of water chemistry conditions examined in this thesis. The results presented in this thesis provide the basis for the development of kinetic-based mechanistic model that may be used by utility operators to evaluate how

changes to water chemistry parameters will affect the dissolution of lead scales present in a drinking water system.

4.2 RECOMMENDATIONS

Improving understanding of lead compounds is required to better estimate and control the dissolution of lead corrosion scales, and thus protect the public. There are many areas associated with lead dissolution in drinking water systems that are still not well understood. For instance, a wide range of values for the equilibrium constant for hydrocerussite and cerussite have been reported in literature. Calculations using these equilibrium constants can result in highly variable estimates of equilibrium total dissolved lead and can introduce high uncertainty into model results. While this study estimated the log equilibrium constant of hydrocerussite to be -15.98 ± 0.53, additional studies are required to more accurately determine the equilibrium constants of these lead (II) carbonates. Within solution, many aqueous lead complexes exist and the accuracy of their equilibrium constants is also uncertain. Further work developing and validating aqueous equilibrium constants would be benefit future thermodynamic modelling efforts. Additional uncertainties exist with regards to the range of stability for both cerussite and hydrocerussite. A review of literature provides an estimated range of stability for cerussite between a pH of 6 and 8; however the exact range is undefined. Work presented in this thesis narrowed this range to between a pH of 7 and 8, however further work determining the precise stability ranges for both cerussite and hydrocerussite is recommended. Accurate knowledge of the boundaries of stability for these lead (II) carbonates would aid the design and analysis of future experimental work, and would also provide recommended operational limits on water chemistries to prevent the destabilization of scales where these phases are dominant.

The kinetics of both the formation and dissolution of cerussite and hydrocerussite are not well understood. The work presented in this thesis represents a step in developing a knowledge base for the dissolution of hydrocerussite. Despite that, experiments are still required to identify the full elementary reactions and mechanisms for both dissolution and formation of the important lead (II) carbonates. Kinetic rate expressions for these should be developed for future work for the calculation of total dissolved lead at consumer point-of-use. Additional work is also required to validate the rate expression developed within this thesis under a wider range of water chemistry conditions. This includes a wider range of pH values and DIC concentrations (including verifying the rate constant at a DIC of 0 mg C/L), and the inclusion of natural organic material, manganese, iodide, chloride, orthophosphate etc. Additional work is also required to investigate the transformation between lead (IV) oxides and lead (II) carbonates under low ORP conditions and varying water chemistry parameters. In this thesis, the effect of free chlorine on hydrocerussite dissolution was explored and a lag phase was observed before chlorine depletion was observed. Although there is speculation with regards to the causes of this lag phase, it is not well understood. Further work is required to explore the causes of this lag and to develop a comprehensive kinetic chlorine decay expression for inclusion in modelling drinking water systems which use a residual free chlorine disinfectant.

The effects of temperature on the stability of lead (IV) oxides or lead (II) carbonates are uncertain. As water distribution pipes are exposed to significant seasonal temperature fluctuations it is recommended future studies examine incorporate temperature effects into equilibrium and kinetic expressions.

To achieve the recommendations provided above, modified or more advanced experimental methods are required. This includes developing a faster sampling/analysis

technique to evaluate dissolution of formation of solid lead phases at <30 second intervals. This is important for quantifying dissolution rates with solid loading concentration of hydrocerussite above 50 mg/L, and may also be required for experiments examining the dissolution or formation of cerussite. An alternative methodology will also need to be developed to quantify the effect of temperature on the kinetic dissolution of lead (II) carbonates to determine the activation energies of these carbonates.

Further knowledge gaps exist with regards to the surface morphology of lead (II) carbonates and lead (IV) oxides within pipes. To develop a complete water chemistry model to estimate the total lead observed at the point-of-use, the surface characteristics will need to be quantified and better understood. This will allow for more accurate calculation of dissolution rates with respect to the available surface area of specific lead solid phases within the pipe.

A. APPENDIX ONE: SUPPLEMENTARY MATERIAL

Reaction	log K	Name
Aqueous Phases		
General		
$H_2O = OH^- + H^+$	-13.997	-
$2 H^+ + 2 e^- = H_2$	-3.15	-
$2H_2O = O_2 + 4H^+ + 4e^-$	-85.9951	-
General - Carbonate		
$2H^+ + CO_3^{-2} = H_2CO_3$	16.681	-
$H^+ + CO_3^{-2} = HCO_3^-$	10.329	-
$Na^+ + CO_3^{-2} = NaCO_3^-$	1.27	-
$Na^+ + H^+ + CO_3^{-2} = NaHCO_3$	10.079	-
Lead Hydroxides		
$Pb^{+2} + H_2O = PbOH^+ + H^+$	-7.597	-
$Pb^{+2} + 2H_2O = Pb(OH)_2 + 2H^+$	-17.094	-
$Pb^{+2} + 3H_2O = Pb(OH)_3^- + 3H^+$	-28.091	-
$2Pb^{+2} + H_2O = Pb_2OH^{+3} + H^+$	-6.397	-
$3Pb^{+2} + 4H_2O = Pb_3(OH)_4^{+2} + 4H^+$	-23.888	-
$Pb^{+2} + 4H_2O = Pb(OH)_4^{-2} + 4H^+$	-39.699	-
$4Pb^{+2} + 4H_2O = Pb_4(OH)_4^{+4} + 4H^+$	-19.988	-
Lead Nitrates		
$Pb^{+2} + NO_3^- = PbNO_3^+$	1.17	-
$Pb^{+2} + 2NO_3^- = Pb(NO_3)_2$	1.4	-
Lead Carbonates		
$Pb^{+2} + 2CO_3^{-2} = Pb(CO_3)_2^{-2}$	9.938	-
$Pb^{+2} + CO_3^{-2} = PbCO_3$	6.478	-
$Pb^{+2} + CO_3^{-2} + H^+ = PbHCO_3^+$	13.2	-
Solid Phases		
Primary Lead Carbonates		
$Pb_3(OH)_2(CO_3)_2 + 2H^+ = 3Pb^{+2} + 2H_2O + 2CO_3^{-2}$	-18.7705	Hydrocerussite
$PbCO_3 = Pb^{+2} + CO_3^{-2}$	-13.13	Cerussite
Other Lead Carbonates		
$Pb_2OCO_3 + 2H^+ = 2Pb^{+2} + H_2O + CO_3^{-2}$	-0.5578	-
$Pb_3O_2CO_3 + 4H^+ = 3Pb^{+2} + CO_3^{-2} + 2H_2O$	11.02	-
$Pb_{10}(OH)_6O(CO_3)_6 + 8H^+ = 10Pb^{+2} + 6CO_3^{-2} + 7H_2O$	-8.76	-
Gaseous Phases		
$O_2 + 4H^+ + 4e^- = 2H_2O$	83.0894	$O_2(g)$
$CO_2 + H_2O = 2H^+ + CO_3^{-2}$	-18.147	$CO_2(g)$

TABLE A.2: SPECIATED EQUILIBRIUM CONCENTRATIONS FROM SELECT EXPERIMENTS FOR EXPERIMENTAL LOGK

DETERMINATION FOR HYDROCERUSSITE

| pH (---)	DIC (mg C/L)	Pb+2 (mol/L)	CO3-2 (mol/L)	Log K (---)
8.00	20.00	3.46E-08	1.06E-05	-16.34
8.00	20.00	3.69E-08	1.06E-05	-16.25
8.00	20.00	3.46E-08	1.06E-05	-16.34
9.00	20.00	2.36E-09	1.01E-04	-15.87
9.00	20.00	2.39E-09	1.01E-04	-15.86
9.00	20.00	2.50E-09	1.01E-04	-15.80
10.00	20.00	2.56E-10	6.28E-04	-15.18
10.00	20.00	2.63E-10	6.28E-04	-15.15
10.00	20.00	2.74E-10	6.28E-04	-15.09
8.00	10.00	6.65E-08	2.60E-06	-16.70
8.00	10.00	7.26E-08	2.60E-06	-16.59
8.00	10.00	6.75E-08	2.60E-06	-16.68
8.00	50.00	2.47E-08	2.72E-05	-15.96
8.00	50.00	2.42E-08	2.72E-05	-15.98
8.00	50.00	2.49E-08	2.72E-05	-15.94
			Average	**-15.98**
			Std. Dev.	**0.53**
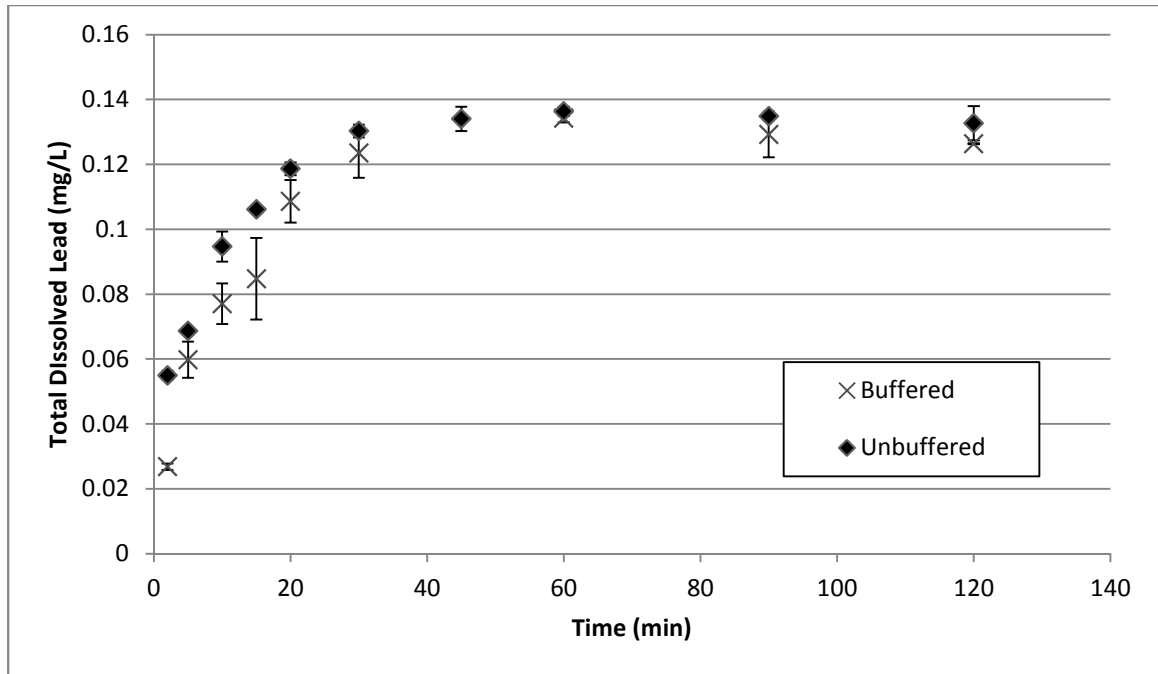
FIGURE A.1: COMPARISON OF BUFFERED (EXP. 1) VS UNBUFFERED (EXP. 10) HYDROCERUSSITE DISSOLUTION EXPERIMENTS (PH 8, DIC 20 MG C/L, IS 0.01 M)
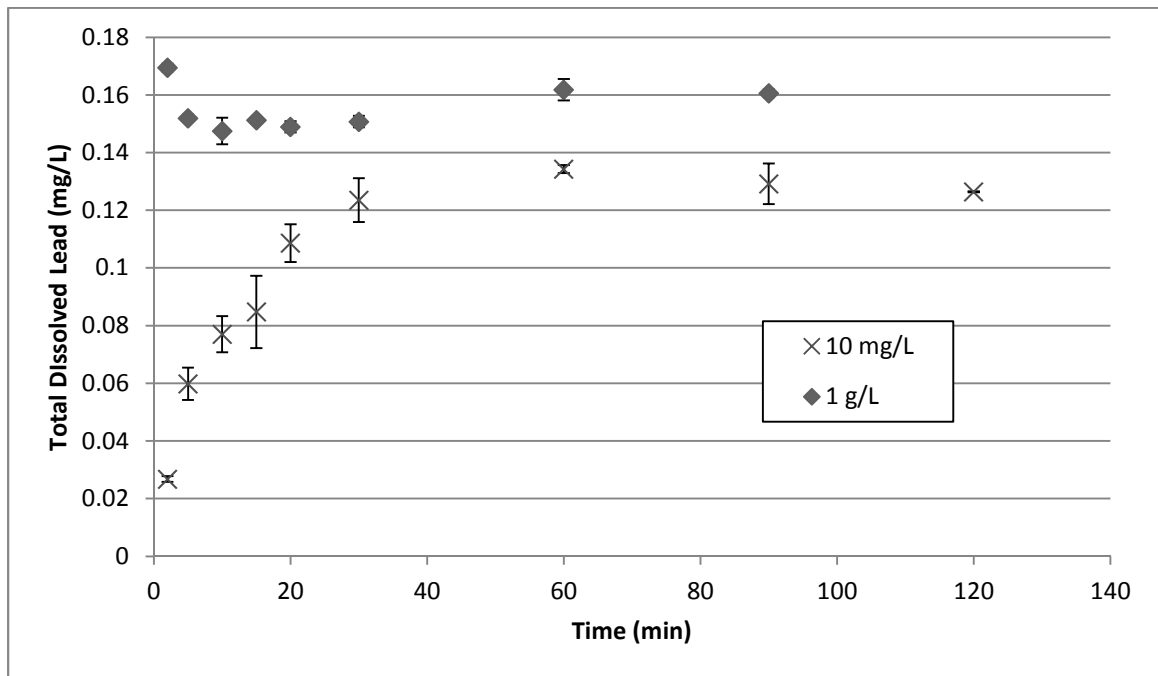

FIGURE A.2: INFLUENCE OF INITIAL SOLID LOADING CONCENTRATIONS ON TOTAL DISSOLVED LEAD FOR HYDROCERUSSITE DISSOLUTION EXPERIMENTS (EXP. 1,10; PH 8, DIC 20 MG C/L, IS 0.01 M).

REFERENCES

1.   Allison, J.D., D.S. Brown, and K.J. Novo-Gradac, *MINTEQA2/PRODEFA2 Version 4 - A geochemical assessment model for environmental systems*, O.o.R.a.D. Environmental Research Laboratory, Editor. 1991, United States Environmental Protection Agency (U.S. EPA): Athens, Georgia. p. 106.

B. Appendix Two: Curriculum Vitae

Caitlin Kushnir, B.Eng.

SUMMARY

Environmental consulting experience primarily encompasses management of contaminated site characterization programs for the oil and gas industry. Much of this work has included Phase I and II Environmental Site Assessments, comprehensive soil and groundwater quality monitoring and site assessment programs, soil remediation activities, and technical report writing. Since returning to school, focus has been on examining and modelling the behavior of lead corrosion scales under various conditions.

WORK EXPERIENCE

20012 – 20124 **Enrolled in M.Sc. program at the University of Western Ontario**

2008 – 2012 **Geo-Environmental Engineer, WorleyParsons, Saskatoon, SK**
Groundwater Monitoring and Reporting, AB, SK & MB
Involved the completion of comprehensive groundwater monitoring programs according to recommendations or the facilities' Environmental approval. Responsibilities included:

- program organization (including scope and budget preparation);
- various field work activities;
- post program site clean up (including contaminated groundwater disposal);
- daily management of costs; and
- preparation of final reports for both the client and regulatory bodies.

Limited Phase I and Monitoring Program
Undertook a Phase I site assessment. Responsible for program organization and site reconnaissance, as well as the gathering, analysis, and interpretation of historical information. These responsibilities culminated in the preparation of a final report.

Phase II Investigations, SK & MB
Undertook Phase II site characterizations at multiple sites. Responsible for the:

- program organization (including scope and budget preparation, and pre-site ground disturbance);
- supervision of multiple subcontractors;
- proper abandonment or installation of piezometers (using rotary drill rigs);
- soil and groundwater sampling (and occasionally Petro FLAG analysis);
- post program site clean up (including contaminated cuttings disposal);
- daily management of costs and scopes; and
- preparation of summary and final reports for the client and regulatory bodies.

Western Monitoring Program
Responsible for the set up, execution and co-ordination of a large scale complex monitoring program (31 sites over 5 provinces).

Soil Vapor Installation and Monitoring
Assisted in the installation and development of several soil vapor monitoring wells. Responsibilities included the supervision of drilling crews, public communication, preparation and installation of monitoring wells, development and construction of routine monitoring equipment, and routine soil vapor monitoring.

Geophysical Assessment
Collected data with regards to ERT, EM31 and EM35 surveys for the contaminant delineation program.

Spill Assessment and Contaminated Soil Removal
Conducted remedial activities through the removal of hydrocarbon impacted materials. Responsible for site characterization and on site confirmatory soil sampling. Analysis and interpretation of data and preparation of a summary report for client.

2006 – 2007 **Environmental Technician, Jagger Hims Ltd., Newmarket, Ont.**
Responsibilities included: acquiring and verifying supporting data for engineering design and decision making; preparing portions of final and preliminary Phase I and Phase II reports; routine flow monitoring of discharge pipes and streams from a large operational quarry to meet regulatory requirements; and confirmatory soil sampling with hand auger.

EDUCATION

- M.Sc. Candidate, University of Western Ontario, 2014
- One Semester M.Eng., University of Western Ontario, 2013
- Bachelors of Engineering, Honours in Environmental Engineering, University of Guelph, Guelph Ontario, 2008

AWARDS

William E. and Ruth Lardner Graduate Award, University of Western, 2014
John Booker Award, University of Western, 2013
Helen Grace Tucker Award, University of Guelph, 2008

CONFERENCES

- *CWN Conference, Ottawa Ontario, March 2015*
  Influence of water chemistry parameters on the dissolution rate of the lead (II) carbonate hydrocerussite
- CWWA Conference, Gatineau Quebec, October 2014
  Development of a semi-kinetic model to evaluate a lead (II) carbonate dissolution in water distribution systems
- OWWA Conference, London Ontario, May 2014
  Poster Title: Equilibrium Geochemical Model to Evaluate Lead Dissolution and Corrosion Scale Transformations in Water Distribution Systems
- Western Environment and Sustainability Conference, March 2014
  Poster Title: Equilibrium Geochemical Model to Evaluate Lead Dissolution and Corrosion Scale Transformations in Water Distribution Systems
- CAWQ Conference, Kingston Ontario, October 2013
  Poster Title: Equilibrium Geochemical Model to Evaluate Lead Dissolution and Corrosion Scale Transformations in Water Distribution Systems
- SyNRGS Conference, University of Western, Ontario, August 2013
  Poster Title: Equilibrium Geochemical Model to Evaluate Lead Dissolution and Corrosion Scale Transformations in Water Distribution Systems
- CWN Conference, Ottawa Ontario, March 2013
  Poster Title: Equilibrium Geochemical Model to Evaluate Lead Dissolution and Corrosion Scale Transformations in Water Distribution Systems